GEOLOGICA CARPATHICA, APRIL 2023, 74, 2, 155–179 https://doi.org/10.31577/GeolCarp.2023.06

Petrography of the Upper Miocene sandstones from the North Croatian Basin: Understanding the genesis of the largest reservoirs in the southwestern part of the Pannonian Basin System

MARIO MATOŠEVIĆ[1,✉], FRANE MARKOVIĆ[2], DIJANA BIGUNAC[3], SANJA ŠUICA[1], KREŠIMIR KRIZMANIĆ[1], ADALETA PERKOVIĆ[1], MARIJAN KOVAČIĆ[2] and DAVOR PAVELIĆ[4]

[1]INA – Industrija nafte d.d., Exploration & Production, Subsurface & Field Development, Exploration & Production Laboratory, Lovinčićeva 4, 10000 Zagreb, Croatia; ✉mario.matosevic@ina.hr
[2]University of Zagreb, Faculty of Science, Department of Geology, Division of Mineralogy & Petrology, Horvatovac 95, 10000 Zagreb, Croatia
[3]INA – Industrija nafte d.d., Exploration & Production, Subsurface & Field Development, Subsurface, Avenija Većeslava Holjevca 10, 10000 Zagreb, Croatia
[4]University of Zagreb, Faculty of Mining, Geology and Petroleum Engineering, Pierottijeva 6, 10000 Zagreb, Croatia

(Manuscript received July 15, 2022; accepted in revised form March 6, 2023; Associate Editor: Ján Soták)

Abstract: This paper presents a petrographic study of the Upper Miocene sandstones from exploration wells in the Sava and Drava Depressions in the North Croatian Basin (SW of the Pannonian Basin System), Central Europe. These sandstones represent the most important reservoir rocks for oil and gas in Croatia. A total of 130 core samples from depths of more than 3000 m were examined. The sandstones generally have a feldspatho–litho–quartzose (fLQ) composition. The modal composition of samples from the Sava Depression is $Q_{39.2–61.0}F_{8.9–26.0}L_{26.1–42.3}$, and $Q_{40.6–63.5}F_{6.6–23.3}L_{20.9–42.3}$ for those from the Drava Depression. Lithic fragments are dominated by extrabasinal carbonates with subordinate metamorphic grains (mostly schists) and less frequent magmatics (granitoids). Garnet, tourmaline, apatite, rutile, epidote, clinozoisite, zoisite, titanite, zircon, staurolite, and opaque minerals form the heavy mineral association and imply an area of provenance dominated by metamorphic rocks. The tectonic setting of the sandstones corresponds to recycled orogen, i.e., a subduction complex or fold-thrust belt. There are no significant compositional differences between the sandstone samples from the two depressions, thus indicating a common main source area and similar diagenetic processes in the subsurface. The sandstones originated from eroded parts of the uplifted Alpine–Carpathian fold belt and are distinct from the Lower and Middle Miocene sandstones in the North Croatian Basin. Observed variations in the sandstones' composition with regards to geographic location and depth are associated with variations in the erosion of parent rocks, including subsequent modification of detrital sediment during transport, mixing, and deposition, as well as burial diagenesis. The Sava and Drava Depressions were part of Lake Pannon in the Late Miocene with no significant topographical obstacles between them for the inflow of the detritus. The study will therefore help with the correlation of the Upper Miocene reservoir rocks in various parts of the North Croatian Basin (as well as adjacent parts of the Pannonian Basin System) and thereby assist with future hydrocarbon exploration in this area.

Keywords: petrography, sedimentary provenance, sandstone reservoirs, Late Miocene, Pannonian Basin System

Introduction

Petrography is a fundamental method in sedimentary provenance studies and remains the prevailing geological approach for understanding the generation of sediments, i.e., their modifications during erosion, transport, deposition, and subsequent diagenesis (e.g., Dickinson et al. 1983; Weltje et al. 1998; Garzanti 2016, 2019; Augustsson 2021). Since the primary composition of source rocks in hinterlands affects the final petrographic composition of sediment in a sedimentary basin (Suttner et al. 1981; Bhatia 1983; Pettijohn et al. 1987; Armstrong-Altrin & Verma 2005; Garzanti 2016, 2019) and plays a major role in sediment behaviour during burial diagenesis affecting its petrophysical parameters (e.g., Ehrenberg 1990; Worden et al. 2018; Lawan et al. 2021), petrography is crucial for estimating reservoir development and quality (Worden et al. 1997, 2018; Worden & Burley 2003; Gier et al. 2008; Rahman & Worden 2016; Lawan et al. 2021). In addition to well-log and seismic data interpretation and integration, petrography persists as an indispensable method in hydrocarbon exploration, contributing to better-quality correlation and modelling of sediments and their properties in the subsurface.

The main goal of sedimentary provenance analysis is to reconstruct and interpret the geology of a source area and to connect the final burial of a detritus with the initial erosion of parent rocks (Ibbeken & Schleyer 1991; Weltje & von Eynatten 2004). Petrography is the only method used in sandstone provenance analysis that simultaneously provides both mineralogical and textural data of sandstones and their forming

constituents (small-scale originals of their parent rocks), thereby allowing direct visualization and reconstruction of the source area (Garzanti 2016). Detrital modes of sandstones can be related to the plate-tectonic setting of a sedimentary basin they were deposited in (Dickinson & Suczek 1979; Dickinson et al. 1983; Dickinson 1985; Weltje & von Eynatten 2004; Weltje 2006) and can reflect the nature of the source terranes, as well as the tectonostratigraphic level achieved by erosion in space and time (Garzanti 2016).

Neogene rocks are the main hydrocarbon deposits of the Pannonian Basin System (PBS). They account for more than 80 % of all reservoirs reported in this area – sandstones constitute 95 % of this, with 90 % being of Miocene age (Dolton 2006). Hydrocarbon generation was triggered by a high geothermal gradient during the initial and subsequent thermal subsidences of the basin (Saftić et al. 2003). The most important reservoir rocks of the PBS in Croatia are the Upper Miocene sandstones, which had been formed through the mechanism of lacustrine cyclic turbidite deposition associated with the progradation of delta systems in Lake Pannon (Magyar et al. 1999, 2013; Ivković et al. 2000; Saftić et al. 2003; Kovačić et al. 2004; Kovačić & Grizelj 2006; Vrbanac et al. 2010; Malvić & Velić 2011; Sztanó et al. 2013, 2015; Balázs 2017; Balázs et al. 2018; Sebe et al. 2020; Anđelković & Radivojević 2021). In the North Croatian Basin (NCB), these sandstones exhibit high values of porosity and permeability. The porosity is usually in the range of 10 % to more than 35 %, with permeability between 0.01 to 1000 mD (Vrbanac et al. 2010; Velić et al. 2012; Kolenković Močilac et al. 2022).

This paper presents a petrographic study of the Upper Miocene sandstones in the NCB (SW part of the PBS), the largest reservoirs of oil and gas discovered in Croatia. Although the basin is a relatively mature petroleum province that has been studied for several decades (e.g., Lučić et al. 2001; Saftić et al. 2003; Dolton 2006; Vrbanac et al. 2010; Malvić & Velić 2011; Velić et al. 2012; Matošević et al. 2019b,c, 2021; Kolenković Močilac et al. 2022), the reservoir properties of the sandstones themselves are not well-known. These sandstones not only continue to be of great interest to the oil industry both in terms of new exploration and the development of existing oil fields, but also in terms of the energy transition, including carbon capture, utilization, and storage, and geothermal energy (cf. Sneider 1990; Alcalde et al. 2019; Davies & Simmons 2021; Willems et al. 2021). Understanding of the primary composition of sandstone reservoir rocks and the factors which influence their petrophysical characteristics is the first step toward reservoir quality evaluation and prediction (Worden et al. 1997, 2018; Worden & Burley 2003; Rahman & Worden 2016; Lawan et al. 2021).

For this study, petrographic analyses were performed on sandstone samples from exploration wells in the Sava and Drava Depression, which are the two largest depressions in the NCB. The paper aims to determine the petrographic composition of the sandstones, compare the samples from the two depressions, interpret their provenance areas, and assess their variability in terms of geographic location and depth. The results will contribute to further exploration of the area and, in particular, to the improved correlation of the Upper Miocene sandstones in the Croatian and adjacent parts of the PBS.

Geological background

The Miocene PBS, which is surrounded by the Alps, the Carpathians, and the Dinarides (Fig. 1), is paleogeographically related to the area of the Central Paratethys. During the Miocene, the connection of the Central Paratethys with the world ocean had been established and ceased several times. The final isolation of the Central Paratethys commenced some 11.6 Ma ago (Steininger & Rögl 1979; Rögl & Steininger 1983; Rögl 1998; Magyar et al. 1999; Harzhauser et al. 2007; Piller et al 2007; Harzhauser & Mandic 2008; Kováč et al. 2017, 2018; Magyar 2021). The nature of the Central Paratethys evolution and the occurrences of endemic faunas have thus necessitated the establishment of regional Miocene stages (Fig. 2).

The SW part of the PBS, which covers almost the entire area of northern Croatia, is represented by the NCB (Figs. 1 and 3). The NCB is elongated, with a WNW–ESE-trending direction and includes several depressions which are bordered by mountains (Pavelić & Kovačić 2018; Figs. 1 and 3). The two largest are the Sava Depression (SD) along the southern edge of the basin, and the Drava Depression (DD) along the northern edge of the basin. These depressions represent river lowlands on the modern surface and, as border areas between Croatia and neighbouring countries, are of vast ecological and economic importance. The maximum depth prior to the pre-Miocene bedrock is 5500 m in the SD and 7000 m in the DD (Prelogović 1975; Pavelić 2001; Saftić et al. 2003; Horváth et al. 2006; Malvić 2011; Malvić & Cvetković 2013). Miocene siliciclastic sediments of the NCB unconformably cover strongly tectonized Paleozoic, Mesozoic, and Paleogene basements, and were deposited from the Early to the Late Miocene in marine, brackish, and freshwater environments (Pamić 1999; Pavelić 2001; Saftić et al. 2003; Pavelić & Kovačić 2018; Šuica et al. 2022a,b).

The development of the PBS began in the Early Miocene as a result of continental collision and subduction of the Eurasian plate under the African (Apulian) plate, including other continental fragments from the south that caused thermal perturbation of the upper mantle, thereby resulting in the weakening and extension of the crust and formation of a back-arc type sedimentary basin (Royden 1988; Horváth 1993, 1995; Kováč et al. 1998; Pavelić 2001; Matenco & Radivojević 2012; Horváth et al. 2015; Balázs et al. 2016; Pavelić & Kovačić 2018). The first stage of the PBS development was characterized by tectonic thinning of the crust and isostatic subsidence, with sedimentary environments changing from continental to fully marine (syn-rift phase; Royden 1988; Tari et al. 1992). The second stage was characterized by reduced tectonic influence, termination of rifting, and subsidence caused by

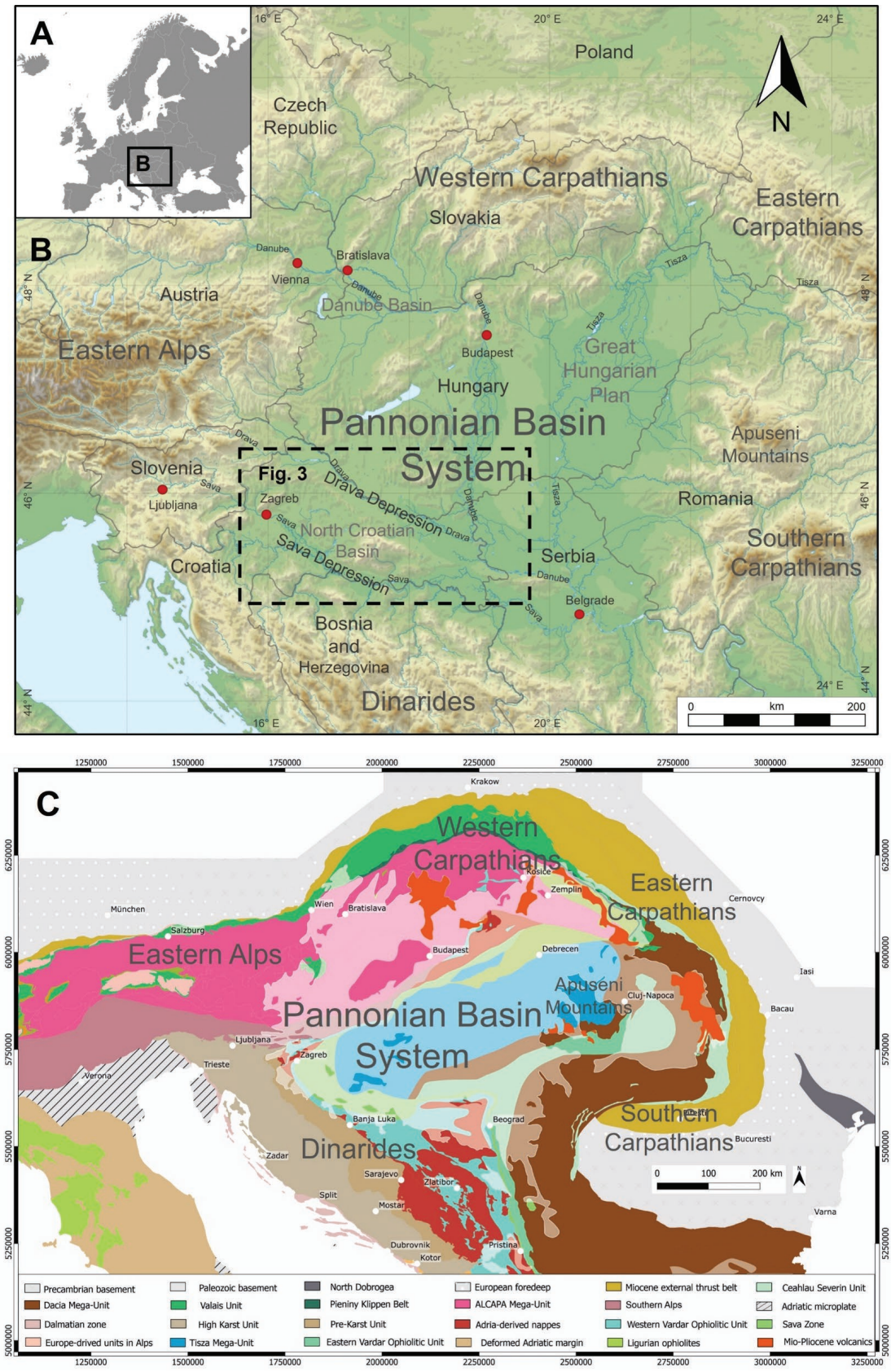

Fig. 1. A — Europe with the geographic position of the Pannonian Basin System. **B** — The location of the Sava and Drava Depressions in the SW part of the Pannonian Basin System (North Croatian Basin) surrounded by the mountain ranges of the Alps, the Carpathians, and the Dinarides. **C** — Modified schematic presentation of the main tectonic units of the region (after Schmid et al. 2008, 2020).

cooling of the lithosphere, with gradual isolation of the PBS from marine influences of the Central Paratethys (post-rift phase; Royden 1988; Tari et al. 1992; Fig. 2). The transition from the syn-rift to the post-rift phase was diachronous through the PBS (Matenco & Radivojević 2012). The final isolation happened approximately 11.6 Ma ago when the large and long-lived Lake Pannon, which existed from the Late Miocene to the Early Pliocene, was formed (Magyar et al. 1999; Harzhauser & Piller 2007; Piller et al. 2007; Mandic et al. 2015). In the NCB, the main hydrocarbon source rocks are represented by the Middle Miocene late syn-rift and early post-rift marine deposits (Badenian and Sarmatian mudrocks), as well as the Upper Miocene early post-rift lacustrine deposits (early Pannonian mudrocks; Barić et al. 2000; Lučić et al. 2001; Saftić et al. 2003; Troskot-Čorbić et al. 2009; Zečević et al. 2010; Matošević et al. 2019a).

The sandstones that later became significant oil and gas reservoirs were formed during the post-rift phase as prograding systems of delta environments within Lake Pannon, which were associated with turbidites in deeper parts of the lake (Juhász 1994; Magyar et al. 1999; Ivković et al. 2000; Saftić et al. 2003; Kovačić & Grizelj 2006; Vrbanac et al. 2010; Malvić & Velić 2011; Sztanó et al. 2013, 2015; Balázs et al. 2018; Sebe et al. 2020; Anđelković & Radivojević 2021). Relatively slow thermal subsidence of the PBS without significant tectonic activity in the Late Miocene (Horváth & Royden 1981; Ivković et al. 2000; Pavelić & Kovačić 2018) was coupled with uplift and erosion of the surrounding Alpine–Carpathian–Dinaric fold belt. Parts of the belt enabled a huge supply of sediment via large fluvial and deltaic systems to flow into the lake (Bérczi et al. 1988; Szentgyörgyi & Juhász 1988; Juhász 1991, 1994; Saftić et al. 2003; Kovačić et al. 2004; Kovačić & Grizelj 2006; Magyar et al. 2013; Pavelić & Kovačić 2018; Sebe et al. 2020; Anđelković & Radivojević 2021). Great depths in the lake developed due to a high rate of subsidence of the basin and prevailing humid climate (Sztanó et al. 2013; Balázs et al. 2018). These factors led to the accumulation of post-rift deposits in the sedimentary succession of several thousand meters, including large sandstone bodies, with the greatest thickness identified in the central part of the depressions (Juhász 1994; Ivković et al. 2000; Saftić et al. 2003; Kovačić & Grizelj 2006; Malvić & Velić 2011; Sebe et al.

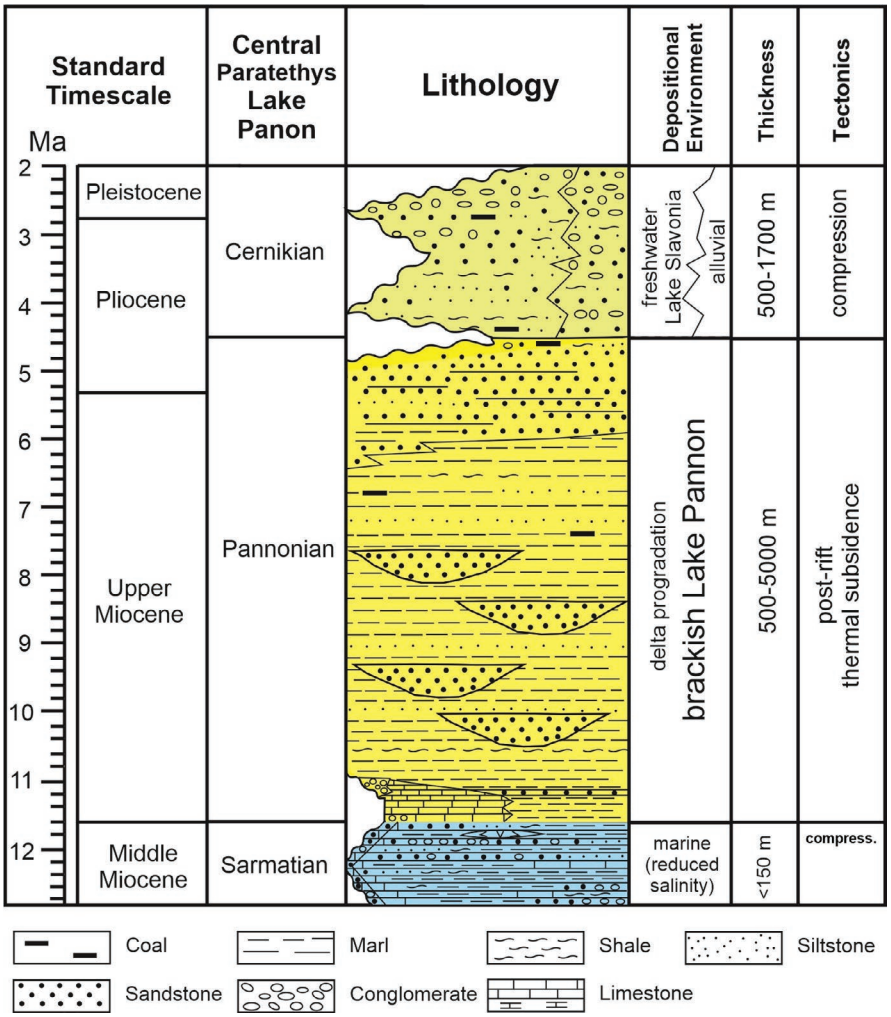

Fig. 2. Stratigraphic scheme of the North Croatian Basin, modified after Saftić et al. (2003), Mandic et al. (2015), and Pavelić & Kovačić (2018).

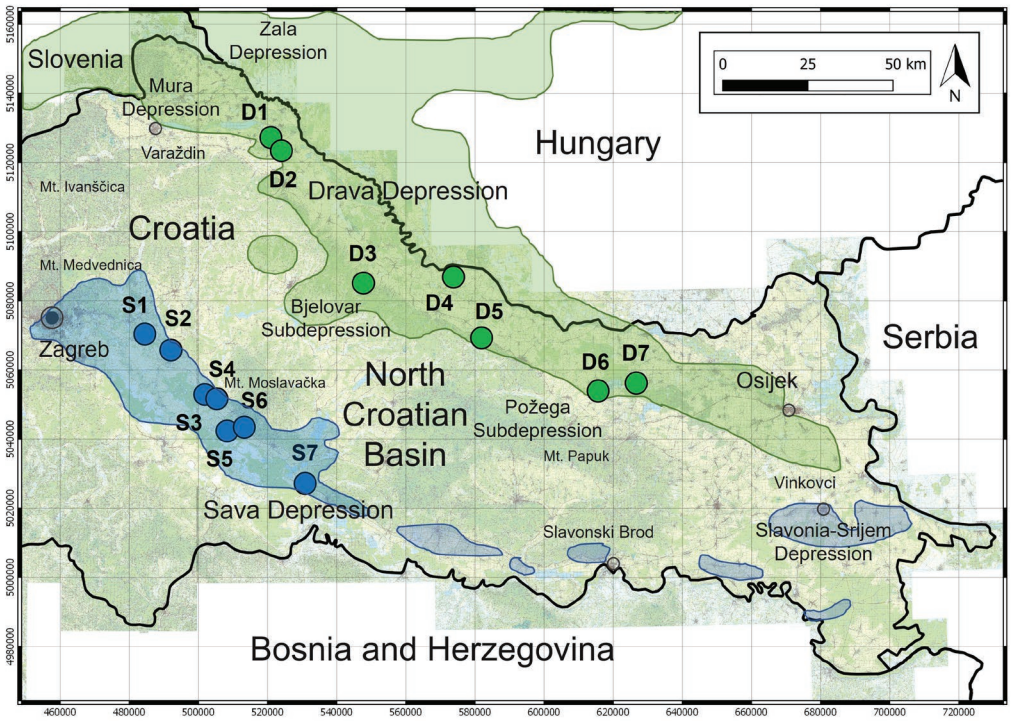

Fig. 3. Position of the North Croatian Basin and locations of exploration wells, which are the subject of this study within the approximate areas of the Sava (S1–S7) and Drava Depression (D1–D7), including neighboring Neogene depressions and sub-depressions.

2020). The thickness of the Upper Miocene deposits in the NCB which, according to regional chronostratigraphy, belong to the Pannonian stage (Hilgen et al. 2012; Mandic et al. 2015; Neubauer et al. 2015; Fig. 2), fluctuates between 2000 m in the western part of the SD to 4000–5000 m along the SW edge of the DD (Saftić et al. 2003). The Pannonian (Upper Miocene) deposits, situated below Cernikian (Pliocene to Pleistocene) lacustrine and alluvial deposits, overlie the Sarmatian (Middle Miocene) marine deposits. (Pavelić 2001; Mandic et al. 2015; Kurečić 2017; Pavelić & Kovačić 2018; Fig. 2). The thickness of the Upper Miocene sandstone bodies varies and is usually in the range of a few meters to several tens of meters, commonly intercalated with mudrocks (layers of siltstones, mudstones, claystones, marls, and shales). The sandstones appear as turbidite mass flow deposits on the slope and basin floor (deeper-water fan lobes, channels, and levees) and are subsequently covered by delta and fluvial system deposits that are morphologically related to regional progradation of the shelf (prodelta, delta front, delta plain and alluvial plain, including distributary channels and mouth bars; Pogácsás 1984; Saftić et al. 2003; Sztanó et al. 2013, 2015). Turbidite systems are restricted to deeper and central parts of the depressions (Sztanó et al. 2015), while delta systems succession and subsequent fluvial deposits are associated with subsequent progradation of the shelf-margin slope (corresponding to clinoforms on seismic profiles; Magyar et al. 2013). The high material inflow in the PBS was mainly from the Alpine–Carpathian source areas, generally following a W/N-NW towards E/S-SE direction (Šćavničar 1979; Ivković et al. 2000; Saftić et al. 2003; Kovačić et al. 2004; Kovačić & Grizelj 2006; Magyar et al. 2013; Sebe et al. 2020). This applies especially to the sources in the ALCAPA tectonic mega-unit of the Eastern Alps and Western Carpathians (e.g., Kuhlemann et al. 2002; Asch 2003; Schmid et al. 2008, 2020). Some explorations of the Upper Miocene sandstones outcropping on the surface in the NCB show that their detritus is of uniform composition, as well as mineralogically and texturally mature (Kovačić et al. 2004, 2011; Kovačić & Grizelj 2006).

The Pliocene and Quaternary are characterized by a transition towards overall compression and structural inversion in the entire NCB (Pavelić 2001; Tomljenović & Csontos 2001). This change is reflected in the formation of many compressional structures and the uplift of basement blocks that formed the present mountains in the area. The uplift was accompanied by strike-slip faulting and counter-clockwise rotation of blocks (Jamičić 1983; Márton et al. 1999, 2002).

Materials and methods

Materials

A total of 130 core samples from the exploration wells drilled by INA – Industrija nafte d.d. were selected and prepared for analyses. The samples included 61 sandstones from seven wells in the SD (Figs. 3 and 4) and 69 sandstones from

seven wells in the DD (Figs. 3 and 4). In order to investigate variations in the sandstones' composition and provenance in both space and time, core samples were taken from wells that covered almost the entire area of the two depressions and were derived from depths ranging from 827.70 m to 3073.90 m in the SD and from 1098.95 m to 4141.15 m in the DD, i.e., covering the entire Upper Miocene succession. The stratigraphic affiliation of the samples was verified by previous biostratigraphic (palynological) analyses, well-log correlation, and seismic interpretation of key horizons representing regional stratigraphic tops, performed in the INA – Industrija nafte d.d. The sampled sandstones were macroscopically homogenous and massive and were selected from relatively thick beds which represent major reservoir units. Samples without significant sedimentary structures (such as erosional, depositional, and post-depositional structures, and bioturbations) and which were of similar grain size were chosen to avoid significant inter-sample variations.

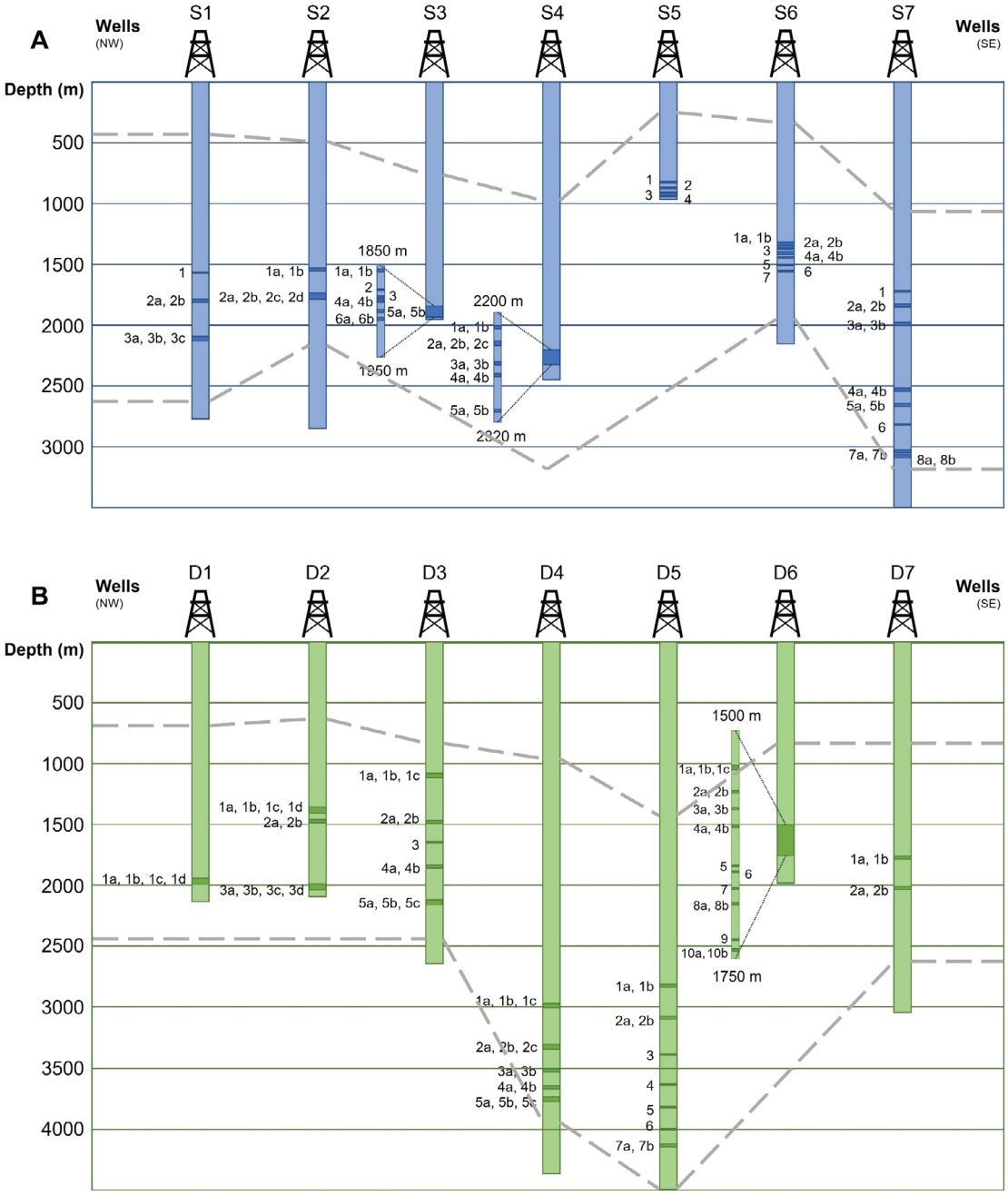

Fig. 4. Positions of the Upper Miocene sandstones' samples from the exploration wells of the Sava (**A**) and Drava (**B**) Depressions. The stratigraphic correlation of the wells is based on the well-log data boundaries between the Upper Miocene (Pannonian) and Pleistocene/Pliocene (Cernikian) in shallower intervals (upper dashed line) and the Upper Miocene (Pannonian) and Middle/Lower Miocene or the Neogene basement in deeper intervals (lower dashed line). For the geographic location of wells, see Fig. 3.

Methods

Petrography

A total of 130 thin sections of sandstones were prepared and analyzed under Olympus BX51 and Leitz Orthoplan polarizing microscopes with an Olympus DP 70 camera and analySIS Five imaging software. The samples were stained with Alizarin Red S according to Evamy & Shearman (1962) to distinguish carbonate minerals (calcite and dolomite), while some were impregnated with blue dye epoxy. At least 100 grains per thin section were measured to determine grain size ranges and the average grain size of each sandstone using the Wentworth (1922) scale. The grain sizes were manually measured (both length (the largest diameter) and width (average diameter)), from which the arithmetic means of the grain sizes were calculated. Based on these measurements, an approximation of the average grain size for each sample was deduced. For the grain-matrix size, a cut-off of 20 μm was applied. The measured grain sizes were generally rounded to whole numbers (expressed in intervals of 10 μm). The roundness of grains was visually estimated using graphical determination charts (Powers 1953; Krumbein & Sloss 1963). Grain sorting was estimated according to Jerram (2001). The textural maturity of the sandstones was estimated according to Folk (1951).

The modal composition of the sandstones was determined by examining the relative proportion of the three main components: quartz (Q), feldspars (F), and lithics or rock fragments (L). At least 300 grains per sample were analyzed (except for the D7-2a, due to the small amount of the material). To classify provenance lithotypes, emphasis was placed on detailed microscopic analyses of rock fragments and their textures (Garzanti 2016). The amounts of phyllosilicates (mica and chlorite) and heavy minerals present were also considered; however, they were not included in the classification of the sandstones since they are mostly conditioned by hydraulic sorting and depositional environment. These components were, however, considered part of the abundance of detrital modes. Sandstone classifications were based on modal compositions (Garzanti 2016, 2019), thereby allowing provenance models to be inferred (Dickinson 1985; Weltje 2006; Garzanti 2016; Augustsson 2021).

The QFL detrital mode analyses were performed according to the modification of the Gazzi-Dickinson point-counting method (Dickinson 1970; Ingersoll et al. 1984; Zuffa 1985). Total quartz content (Q or Qt) included all types of monocrystalline (Qm) and all types of polycrystalline quartz (Qp). Polycrystalline quartz (Qp) included polycrystalline quartz grains, all types of polycrystalline tectonic quartz (quartzite), and polycrystalline microcrystalline quartz (cherty grains). Feldspar content (F) included twinned plagioclase feldspar (Pt) and all potassium (alkali) feldspar (i.e., microcline, orthoclase, perthite, and sanidine), non-twinned plagioclase feldspar, sericitized plagioclase feldspar, albitized potassium (alkali) feldspar, and other altered and partly-dissolved plagioclase or potassium (alkali) feldspar, all represented as a single value (K+P). Rock fragments or lithic grains (L) included metamorphic (Lm), magmatic (igneous; Lv), and sedimentary (Ls) rocks. Rock fragments were considered as such only if individual minerals forming the rock fragments were less than 63 μm (e.g., quartz, feldspar, and mica forming a granitoid fragment). Carbonatic clasts were considered rock fragments, regardless of the sizes of individual minerals and/or fossils forming the clast. The share of total rock fragments (Lt; Dickinson 1985) included all types of polycrystalline quartz (Qp), together with tectonic quartz and cherty grains. The modal composition of rock fragments (L), excluding polycrystalline quartz (Qp; Garzanti 2019), along with tectonic quartz and cherty grains, included the content of metamorphic rocks (Lm) with all types of quartz–mica tectonites (TQM) and polycrystalline mica (Mp), the content of magmatic (igneous) rocks (Lv) with extrusive (volcanic) rocks (Lex) and intrusive (plutonic) rocks (Lp), and the content of sedimentary rocks (Ls) with all types of carbonatic (Lcarb) and siliciclastic (Lncarb) sediments. Quartz–mica tectonite grains (TQM) included all types of metapsammite grains, with or without feldspar, and all types of metaigneous grains, along with gneiss and some types of mica schist (including those with more than 25–30 % share of quartz). Polycrystalline mica grains (Mp) included all types of metapelite grains, along with slate, phyllite, some types of mica schist (including those with less than 25–30 % share of quartz), and metamorphic rocks of possible primary volcanic origin as well. Extrusive (volcanic; Lex) grains included all types of extrusive (effusive) grains, along with volcaniclastic rocks (and/or tuffs) and volcanic glass. Intrusive (plutonic; Lp) grains included granitoid rocks, along with microlithic granites, and all types of other intrusive rocks (e.g., diorite, gabbro, etc.). Sedimentary carbonatic grains (Lcarb) included all types of limestones and dolomites (micrite, sparite, grainstone, packstone, wackestone, etc.) and evaporites, along with recrystallized carbonatic grains and metacarbonatic grains, since it was difficult to distinguish diagenetically altered and recrystallized carbonatic rock fragments from e.g., rock fragments of marble, as well as all types of intrabasinal or recycled carbonate bioclasts. Sedimentary siliciclastic grains (Lncarb) included all types of mudrocks (siltstones mudstones, claystones, marls, shales, etc.). Phyllosilicates were grouped separately in the M group, including mica (muscovite, biotite, etc.) and chlorite. Accessory heavy minerals and opaque minerals were grouped in the HM group. Miscellaneous and unidentified grains were grouped in the Misc group, including hardly-recognizable, deformed, and altered (usually dissolved) grains, as well as those that were indeterminable due to other reasons (e.g., knowledge, size, etc.).

SEM & EDS

Scanning electron microscope (SEM) analyses were performed on selected sandstone samples to confirm the features observed using polarizing light microscopes. The morphological characteristics of the sandstones and individual grains,

including their chemical and mineralogical composition, were studied. Particular attention was given to the determination of heavy minerals and rock fragments that were hard to determine by optical microscopes due to the small dimensions or to alteration (e.g., dissolution and recrystallization). SEM analyses were also used to determine types of cement and clay minerals present in intergranular space. The mineral determination relied on the combination of morphological characteristics of a single crystal, which had been acquired with a secondary electron (SE) image, back-scattered electron (BSE) image, and energy-dispersive X-ray spectroscopy (EDS) spectra. X-ray spectra were compared to literature data of known spectra, and a mineral name was assigned to the point of interest (Severin 2004). Measurements were performed on gold-coated samples. Analytical conditions included a high vacuum and a variety of acceleration voltages (5–25 kV), spot sizes (30–50), and magnifications (25–20,000×). Analyses were performed using a JEOL JSM-6510 LV SEM apparatus (JEOL, Tokyo, Japan) equipped with an energy-dispersive X-ray spectroscope using Oxford INCA X-act system (Oxford Instruments, High Wycombe, UK).

Results

Modal composition

In the following section, the results of petrographic analyses of the Upper Miocene sandstones from the wells in the SD and DD are presented. Tables with detailed results of modal compositions for each sample are provided in the Electronic Supplement, which can be found online (Supplementary Tables S1–S14).

The Upper Miocene sandstones from 35 cores from the SD and 33 cores from the DD were examined (Fig. 4). The sandstones have angular to sub-rounded grains with average sizes from 70 to 160 µm in samples from the SD and from 90 to 220 µm in samples from the DD (Suppl. Tables S1–S14). The grains correspond to very fine and fine-grade sand (grain sizes range from 20 to 1200 µm in the SD and from 20 to 1400 µm in the DD). Grains are predominately well- to moderately well-sorted, rarely moderately-well or well-sorted, and in extreme cases, moderately-well to poorly-sorted. They have tangential (point) and, to a lesser extent, concavo-convex and sutured contacts. Sandstones are texturally mature to sub-mature, and rarely exclusively mature or sub-mature.

The framework petrography (QFL modal composition) of the sandstones in the samples from the SD matches the content of Q in the range of 39.2–61.0 % (average: 50.3 %), F 8.0–26.0 % (average: 15.6 %), and L 26.1–42.3 % (average: 34.1 %; Table 1; Figs. 5 and 6). In samples from the DD, the content of Q is 40.6–63.5 % (average: 51.4 %), F 6.6–23.3 % (average: 14.7 %), and L 20.9–42.3 % (average: 33.9 %; Table 1; Figs. 5 and 6). Qm in the SD is in the range of 28.5–48.6 % (average: 37.2 %) and the share of Lt is between 37.6–57.8 % (average: 47.2 %; Table 1). In the DD, Qm is in the range of 28.1–48.7 % (average: 36.5 %) and the share of Lt is between 37.7–60.6 % (average: 48.8 %; Table 1).

The modal composition of rock fragments in samples from the SD is characterized by Lm ranging from 11.6 % to 42.9 % (average: 27.9 %), Lv 4.9–22.1 % (average: 10.0 %), and Ls 43.2–77.7 % (average: 62.1 %; Table 2; Figs. 7 and 8). For samples from the DD, Lm range from 14 % to 41.9 % (average: 28.8 %), Lv 2.2–28.5 % (average: 9.7 %), and Ls 37.4–80.9 % (average: 61.4 %; Table 2; Figs. 7 and 8). In the total modal grain composition of samples from the SD, M accounts for 4.5–23.4 % (average: 15.5 %) and HM for 1.2–6.7 % (average: 3.4 %; Table 1). M accounts for 6.4–26.3 % (average: 15.5 %) and HM for 0.8–6.2 % (average: 3.4 %) in samples from the DD (Table 1).

If considering only the most abundant QFL component (Garzanti 2019), all analyzed sandstones can be classified as quartzose sandstones, except for one sample from S6 which responds to lithic sandstone. Based on the two most abundant QFL components, the sandstones belong to the LQ group and, to a lesser extent, to the QL group (some samples from S6). Similarly, according to the sixfold subdivision (Weltje 2006), the sandstones can be classified as quartzolithic (Ql), and only one sample from S6 as lithoquartzose (Lq) sandstone. According to the expanded scheme of Garzanti (2016), the sandstones can generally be classified as feldspatho–litho–quartzose (fLQ) and less often as litho–quartzose (LQ; some samples from S4, and some samples from D1, D3, and D4) and feldspatho–quartzo–lithic (fQL; one sample from S6; Fig. 6).

Rock fragments

A significant presence of fragments of numerous rock types in the analyzed sandstones was determined in both depressions (Tables 1 and 2; Figs. 5, 7 and 8). The most frequently observed fragments are those of Ls, followed by Lm and Lv (Table 2; Figs. 5, 7 and 8). Lcarb are the dominant type of sedimentary rock fragments, constituting on average 20.8 % of the sum of QFL composition in the SD and 20.5 % in the DD (Figs. 5 and 7; Suppl. Tables S1–S14). They include different types of dolomites and limestones, usually in the form of altered and recrystallized sparite, micrite (mudstone), packstone to grainstone, etc. Lcarb also include possible metamorphosed carbonates (metacarbonate and marble), as well as rarely observed recycled bioclasts, such as fragments of undetermined foraminifera shells, mollusks, and red algae (Fig. 7). The carbonate fragments are more rounded in comparison to other grains (Figs. 5 and 7). Lncarb can be observed to a lesser degree, with an average of only 0.7 % in the sum of QFL composition in both depressions (Suppl. Tables S1–S14). They are usually in the form of mudrocks (mostly marls, claystones to mudstones, shales rich with organic matter, and siltstones) and generally represent deformed rip-up clasts (Figs. 5 and 7). Although imperceptible through the modal composition, fragments of sandstones were also observed during the analyses, albeit in extraordinarily small quantities. Cherty grains are extremely rare (Fig. 7). Lm are very frequent and mostly

Table 1: Modal composition of the Upper Miocene sandstones from the exploration wells of the Sava (S1–S7) and Drava Depression (D1–D7) with minimal, average, and maximal values for the individual component: Q – quartz; Qm – monocrystalline quartz; F – feldspar; L – rock fragments; Lt – total rock fragments (including polycrystalline quartz); M – phyllosilicates; HM – heavy minerals.

Exploration Well (Nr. of Samples)	Q (%)			Qm (%)			F (%)			L (%)			Lt (%)			M (%)			HM (%)		
	Min	Average	Max	Min	Average	Max	Min	Average	Max	Min	Average	Max	Min	Average	Max	Min	Average	Max	Min	Average	Max
S1 (6)	42.4	47.6	51.4	28.5	32.1	34	11.1	13.4	18	34.6	39	41.5	53.1	54.5	57.8	4.5	11.4	17.8	2	3.2	4.6
S2 (6)	47.4	51.7	54.6	37.3	40.2	42.9	11.2	13.3	15.8	31.6	34.9	39.6	43.3	46.4	49.7	6.4	10	14.6	1.7	3.7	6.7
S3 (10)	43	49.1	54.2	30.5	37.5	41.4	15.8	17.4	18.8	27	33.5	39.4	41.5	45.1	52	10.2	15.7	19.7	2.4	3.6	5.9
S4 (11)	48.7	56.3	61	34.4	42.4	48.6	8	11.5	13.4	28.2	32.2	40.3	40.6	46.1	54.6	9.3	15.8	22.6	1.2	2.9	5.8
S5 (4)	46	49.7	51.7	33.1	37.1	40.4	14.2	17.7	22.7	30.1	32.6	34.9	40.4	45.2	52.7	11.1	16.1	20.5	3.8	5.4	6.6
S6 (10)	39.2	46.2	49.4	31.2	34.2	39.1	13.1	17.1	21	29.6	36.6	42.3	42.5	48.6	52.7	10.9	18.6	22.7	1.4	3.4	6.6
S7 (14)	45.9	50	57.9	31.9	36	39.5	12.7	17.8	26	26.1	32.2	38.1	37.6	46.1	53	9.2	16.8	23.4	1.6	3	5
D1 (4)	47.3	48.9	51.4	31.6	33.4	35	9.9	13.9	19	33.7	37.4	42.3	48.1	52.7	55.9	13	15.4	18.7	1.6	2.8	3.8
D2 (10)	46.2	51.2	53.8	29.2	33.9	37.8	10.2	12.3	14.6	32.8	36.5	41	47.6	53.8	60.6	7	13	20.3	1	3.5	6.2
D3 (11)	56.3	58	62.2	37.5	42.7	48.7	6.6	10	14.7	27.1	32	36.7	41.9	47.3	54.5	11.2	16.1	22.6	1.3	2.3	3.7
D4 (13)	49.3	54.3	63.5	33.4	36.7	42.3	9.8	13.3	17.7	20.9	32.4	38	44.5	50	56.8	6.4	14	26.3	1.3	2.8	4.3
D5 (10)	43.5	49.1	52.9	31.4	36.4	40	13.9	16.6	22.2	30.2	34.2	39.7	41.4	46.9	52.8	10.8	15.2	21.2	0.8	2	3.9
D6 (17)	40.6	46.5	49.5	28.1	33.6	37.7	15.4	18.8	23.3	27.8	34.7	39.4	40.5	47.6	54.8	6.8	17.1	21.5	0.8	2.4	4.1
D7 (4)	49.8	53.7	57	39.3	41.2	44.2	13.5	16.7	20.4	24	29.6	34.2	37.7	42.1	47.1	11.5	13.6	16.3	1.1	2.4	5

include mica schists, quartzites, and gneisses, but also metapelites (slates and phyllites) and in extremely rare circumstances, metasandstones (Figs. 5 and 7). TQM group fragments on average constitute 6.1 % of the sum of QFL composition in the SD and 5.7 % in the DD (Suppl. Tables S1–S14). The Mp group on average constitutes 3.5 % of the sum of QFL composition in the SD and 3.7 % in the DD (Suppl. Tables S1–S14). Lv are present to a lesser extent and mainly represented by granitoids (Fig. 7). Due to different intersections of grains, they may in part correspond to metamorphic rocks (gneisses and/or schists). They constitute on average 3.0 % of the sum of QFL composition in the SD and 2.9 % in the DD (Suppl. Tables S1–S14). Lex are far less commonly observed than Lp and include altered volcanic rocks with accompanying volcaniclastics (tuffs) and volcanic glass (Fig. 7). They constitute on average only 0.3 % of the sum of QFL composition in the SD and 0.2 % in the DD (Suppl. Tables S1–S14).

Heavy minerals

Almost the same association of accessory minerals was identified in both depressions. Garnet is the most abundant heavy mineral in the sandstones and is present in all analyzed samples in greater quantities (Figs. 5 and 9). It is followed by apatite, tourmaline, rutile, and zircon (Fig. 9). Minerals of epidote, clinozoisite, and zoisite, as well as staurolite and in rare circumstances, amphibole, are more significantly present in shallower intervals of wells (up to 1000–1500 m), especially in the SD. A small amount of chloritoid and titanite was also observed. SEM and EDS analyses confirmed the heavy mineral association (Fig. 5) detected via optical microscopy and determined additional heavy minerals in extremely small quantities – monazite and barite. The EDS of garnet grains frequently matches the almandine phase. Numerous opaque minerals were also detected with optical microscopy. SEM and EDS analyses of these opaque minerals confirmed that they mostly correspond to iron oxides, hydroxides, and sulfides (magnetite, hematite, goethite, and pyrite).

Compositional changes with the geographic position and depth

Petrographic analyses of the Upper Miocene sandstones revealed trends of relative changes in the modal composition with a change of geographic position and depth (Supplementary Figs. S1–S7). From the W/NW towards the E/SE, both depressions exhibit an increase in F (Suppl. Fig. S1), Lm (Suppl. Fig. S3), and Lv (Suppl. Fig. S3) components, as well as a decrease in Q (Suppl. Fig. S1), L (Suppl. Fig. S1), Lt (Suppl. Fig. S2), and Ls (Suppl. Fig. S3) components. Subgroups of Q, F, Lm, Lv, and Ls further display uniform trends of changes from the W/NW towards the E/SE in both depressions: a decrease in Qp, Lex, Lcarb, and TQM, as well as an increase in all types of K+P, Lp, Lncarb, and Mp. However, a slight decrease in Pt can be detected in the SD, while an increase can be observed in the DD. The decreasing trends of

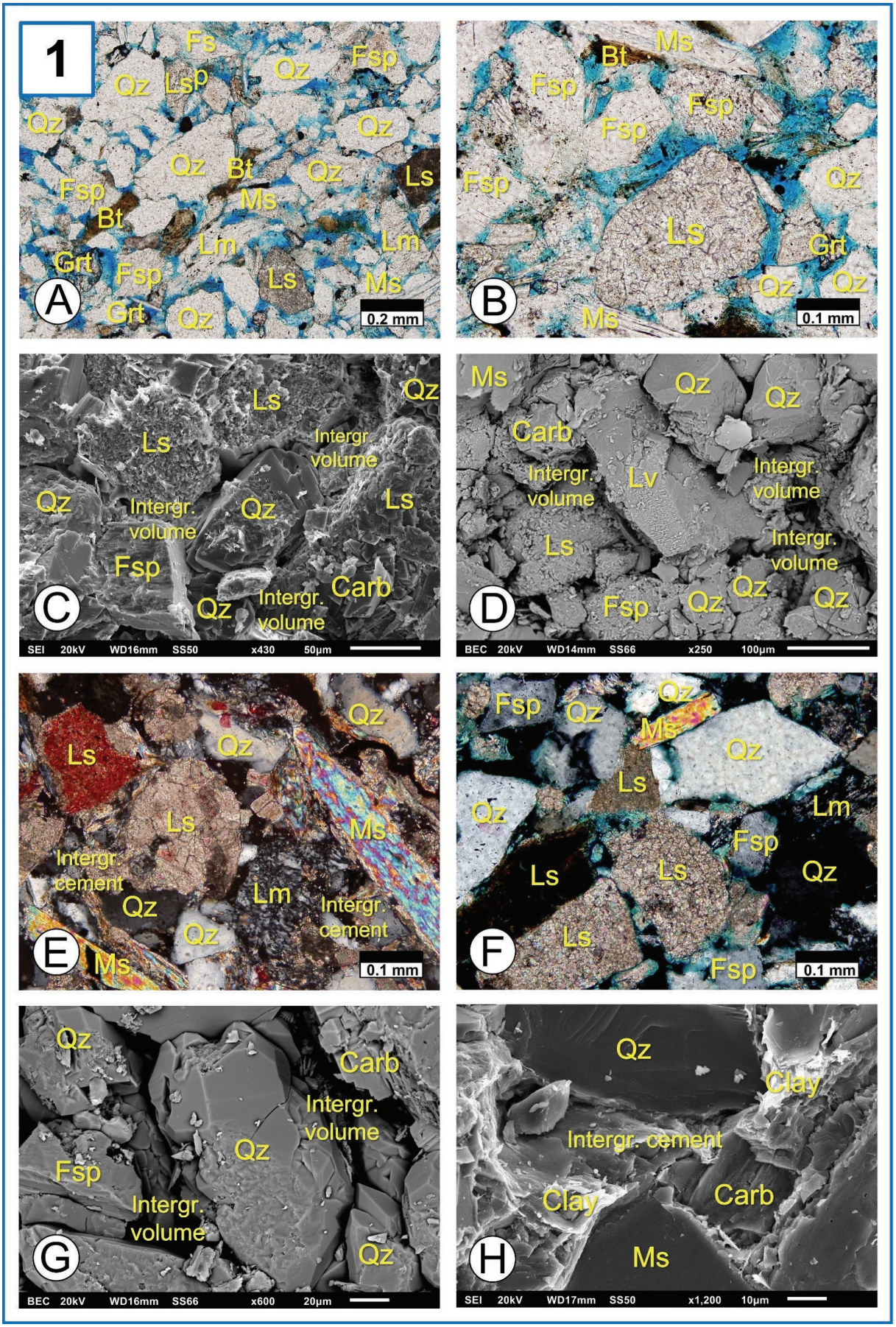
1
Fs
Qz
Lsp
Fsp
Bt
Ms
Lm
Grt
Ls
A
0.2 mm
B
0.1 mm
C
Intergr. volume
Carb
SEI 20kV WD16mm SS50 x430 50µm
D
Lv
BEC 20kV WD14mm SS66 x250 100µm
E
Intergr. cement
F
G
BEC 20kV WD16mm SS66 x600 20µm
H
Clay
SEI 20kV WD17mm SS50 x1,200 10µm

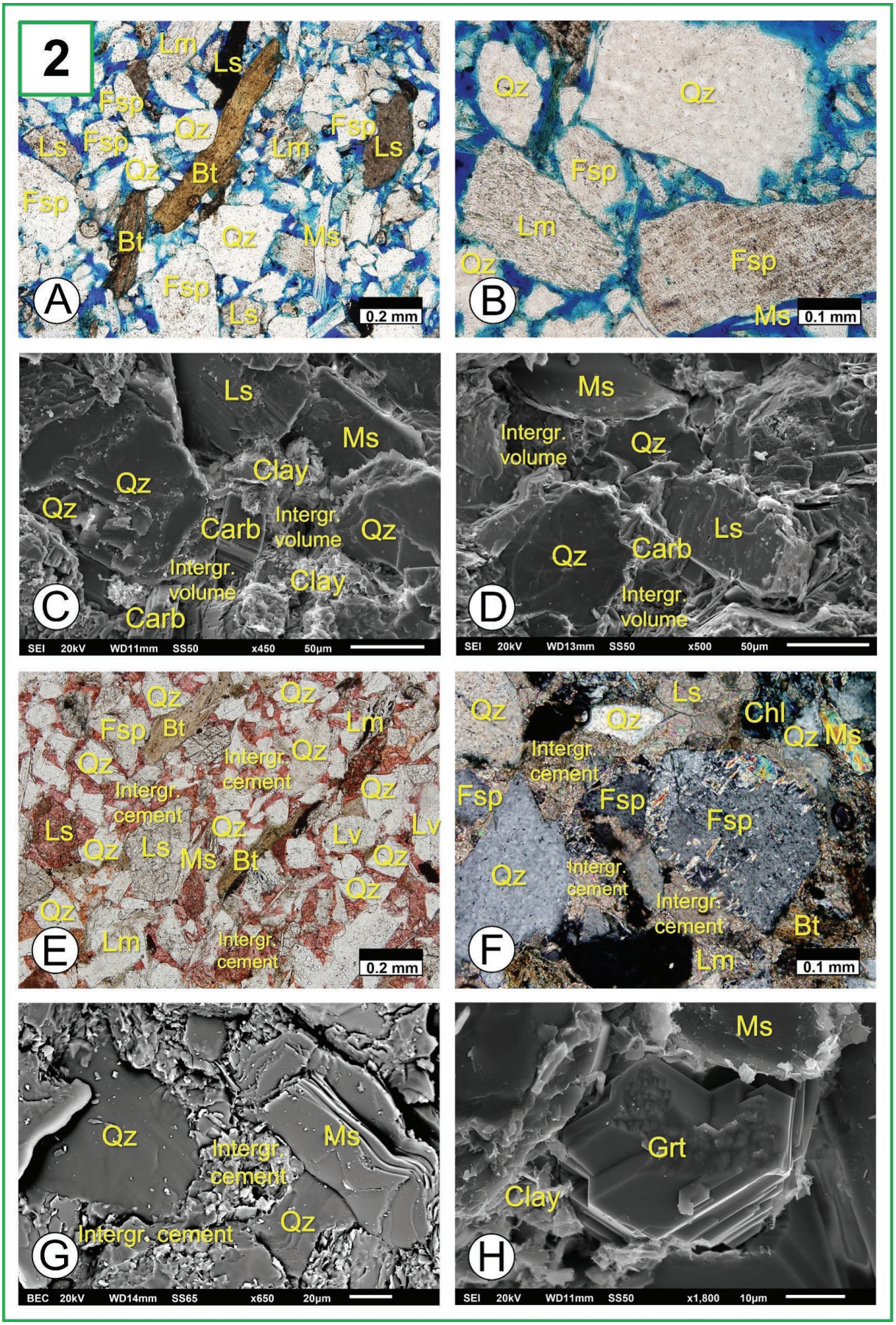
2
Lm
Ls
Fsp
Qz
Fsp
Ls
Fsp
Qz
Lm
Fsp
Ls
Qz
Bt
Fsp
Bt
Qz
Ms
Fsp
Ls
A
0.2 mm
Qz
Qz
Fsp
Lm
Qz
Fsp
Ms
B
0.1 mm
Ls
Ms
Clay
Qz
Qz
Carb
Intergr. volume
Qz
Intergr. volume
Clay
Carb
C
SEI 20kV WD11mm SS50 x450 50µm
Ms
Intergr. volume
Qz
Ls
Qz
Carb
Intergr. volume
D
SEI 20kV WD13mm SS50 x500 50µm
Qz
Qz
Lm
Fsp
Bt
Intergr. cement
Qz
Qz
Intergr. cement
Qz
Ls
Qz
Lv
Lv
Qz
Ls
Ms
Bt
Qz
Qz
Qz
Lm
Intergr. cement
E
0.2 mm
Qz
Ls
Chl
Qz
Ms
Qz
Intergr. cement
Fsp
Fsp
Fsp
Qz
Intergr. cement
Intergr. cement
Bt
Lm
F
0.1 mm
Ms
Qz
Intergr. cement
Ms
Qz
Intergr. cement
G
BEC 20kV WD14mm SS65 x650 20µm
Ms
Grt
Clay
H
SEI 20kV WD11mm SS50 x1,800 10µm

Fig. 5. The Upper Miocene sandstones of the Sava Depression under polarizing light and scanning electron microscope. **(1): A** — Main grains and intergranular volume of the sandstone filled with blue-dyed epoxy showing primary porosity (S3-4b, PPL); **B** — Mineral grains and rock fragments in the sandstone (with rounded carbonatic Ls in the middle; S6-2b, PPL); **C** — Secondary electron image of the sandstones with main grains and intergranular volume (S2-2c, SEM SE); **D** — Backscattered electron image of the sandstone with main grains and intergranular volume (S6-5, SEM BE); **E** — Carbonatic Ls and Lm rock fragments and other grains in the sandstone with carbonate cement in intergranular space (S4-3b, XPL); **F** — The sandstone with primary intergranular porosity under cross-polarized light (S7-1, XPL); **G** — Qz grains and Qz overgrowths on grains and within pores (S1-3a, SEM SE); **H** — Intergranular space of the sandstone filled with cement (combination of carbonate minerals and clays; S7-8a, SEM SE); and the Upper Miocene sandstones of the Drava Depression under polarizing light and scanning electron microscope. **(2): A** — Main grains and intergranular volume of the sandstone filled with blue-dyed epoxy showing primary porosity (D6-10a, PPL); **B** — Mineral grains and rock fragments in the sandstone (Lm on the left; D6-1b, PPL); **C** — Secondary electron image of the sandstones with main grains and intergranular volume partly filled with carbonate minerals and clays (D1-1c, SEM SE); **D** — Main grains in the sandstone and the intergranular space party filled with carbonate cement (D4-2b, SEM BE); **E** — Mineral grains and rock fragments in the sandstone with carbonate cement in intergranular space (D7-2b, PPL); **F** — The sandstone with carbonate cement precipitated between grains (S5-1a, XPL); **G** — Backscattered electron image of the sandstone with main grains and cement (combination of carbonate minerals and clays) in intergranular space (D5-6, SEM BE); **H** — Etched garnet (D1-1c, SEM SE). Qz – quartz, Fsp – feldspar, Lm – metamorphic rock fragment, Lv – magmatic rock fragment, Ls – sedimentary rock fragment, Ms – muscovite, Bt – biotite, Chl – chlorite, Grt – garnet, Carb – carbonate cement. PPL = plane-polarized light, XPL = cross-polarized light, SE = secondary electron image, BE = backscattered electron image. Photo: M. Matošević

Q in both depressions are not overly pronounced (Suppl. Fig. S1). Coincidentally, the SD exhibits almost no changes in Qm from the W/NW towards the E/SE, while a slight increase can be observed in the DD (Suppl. Fig. S2). Increasing trends of F and Lm, as well as the decreasing trends of Lt and Ls are more prominent in the DD (Suppl. Figs. S1–S3). A more pronounced increase in Lv values was detected in D5 (Suppl. Fig. S3). M shows increasing trends from the W/NW towards the E/SE in both depressions. A very slight increasing trend of HM in the SD and a decreasing trend of HM in the DD can also be noticed. The sandstones' grain size from the W/NW towards the E/SE has a decreasing trend in the SD and an increasing trend in the DD.

An increase in Q and Lt components, as well as a decrease in F, L, Lm, and Ls components can be observed in both depressions with the increase of relative depth (Suppl. Fig. S4 and S6). However, a slightly decreasing trend of Lv can be observed in the SD, while an increasing trend can be detected in the DD (Suppl. Fig. S4 and S6). In addition, some sub-groups of Q, F, Lm, and Ls display uniform trends of changes with depth in both depressions: a decrease in K+P, TQM, and Lncarb, as well as an increase in Qp. Trends of Qm, Pt, Mp, and sub-groups of Lv do not coincide between the two depressions. There are no indications of changes with the depth of Lcarb in the SD, while the DD exhibits a decreasing trend of Lcarb. The increasing trend of Q and the decreasing trend of F are more prominent in the SD (Suppl. Fig. S4 and S6). HM shows decreasing trends with depth in both depressions (Suppl. Fig. S5 and S7); however, in the SD, the trend is more noticeable. While the SD exhibits an increase in M with depth, the DD exhibits a decrease in M (Suppl. Fig. S5 and S7). The sandstones' grain size with depth has a decreasing trend in the SD (Suppl. Fig. S5) and an increasing trend in the DD (Suppl. Fig. S7). Furthermore, a mutual connection and dependence of ratios of M and Mp values can be observed in most samples. Changes in HM in relation to changes in M, in the form of an increased share of one in relation to a decreased share of the other and vice versa, were noticed in the samples as well (Suppl. Fig. S5 and S7). A strong bond between the HM component and grain size is also confirmed in the sandstones (Suppl. Fig. S5 and S7) – the smaller the average grain size of the sample, the higher the concentration of HM.

Matrix and cement composition

For samples from both depressions, the intergranular volume of the sandstones is either unfilled, i.e., with empty pores between grains, or is partly or fully filled with carbonate cement and a fine-grained matrix, as well as different types of clay minerals (Fig. 5).

SEM and EDS analyses confirmed the matrix and cement composition of the sandstones. Carbonate cement largely matches calcite and ankerite (Fig. 5). The fine-grained matrix occurs as a combination of carbonate minerals (including calcite, dolomite, and ankerite), quartz, mica, and feldspar (Fig. 5). Different types of detrital and authigenic clay minerals were determined as well in the samples – kaolinite, illite, chlorite, and different types of interstratified clays (Fig. 5). Silica cement was also frequently observed, usually in the form of quartz overgrowths on the main quartz grains (Fig. 5).

Discussion

The Upper Miocene sandstones from the SD and DD are compositionally very similar. The sandstones' most abundant rock fragments are carbonate sedimentary rocks, mica schists, quartzites, gneisses, and granitoid rocks. Although the composition of the HM assemblage could have been modified by diagenesis, similar HM association of the Upper Miocene sandstones was earlier detected on the surface and in deep exploration wells in the NCB (Šćavničar 1979; Kovačić & Grizelj 2006). Therefore, it can be proposed that HM, along with rock fragments, reflects the composition of the source area. The majority of HM in the sandstones could have been derived from two groups of parent rocks: low and medium-grade dynamo-thermal metamorphic and felsic to

intermediate igneous rocks (either as primary minerals or alteration products). One portion of HM is resistant to weathering and transport (e.g., rutile, tourmaline, zircon, barite) and could also have recycled sedimentary origin. Other than limestones and dolomites, which have no influence on the HM content, the composition of rock fragments corresponds to rocks that could be sources of the HM assemblage. It is thus reasonable to conclude that sandstones from the SD and DD

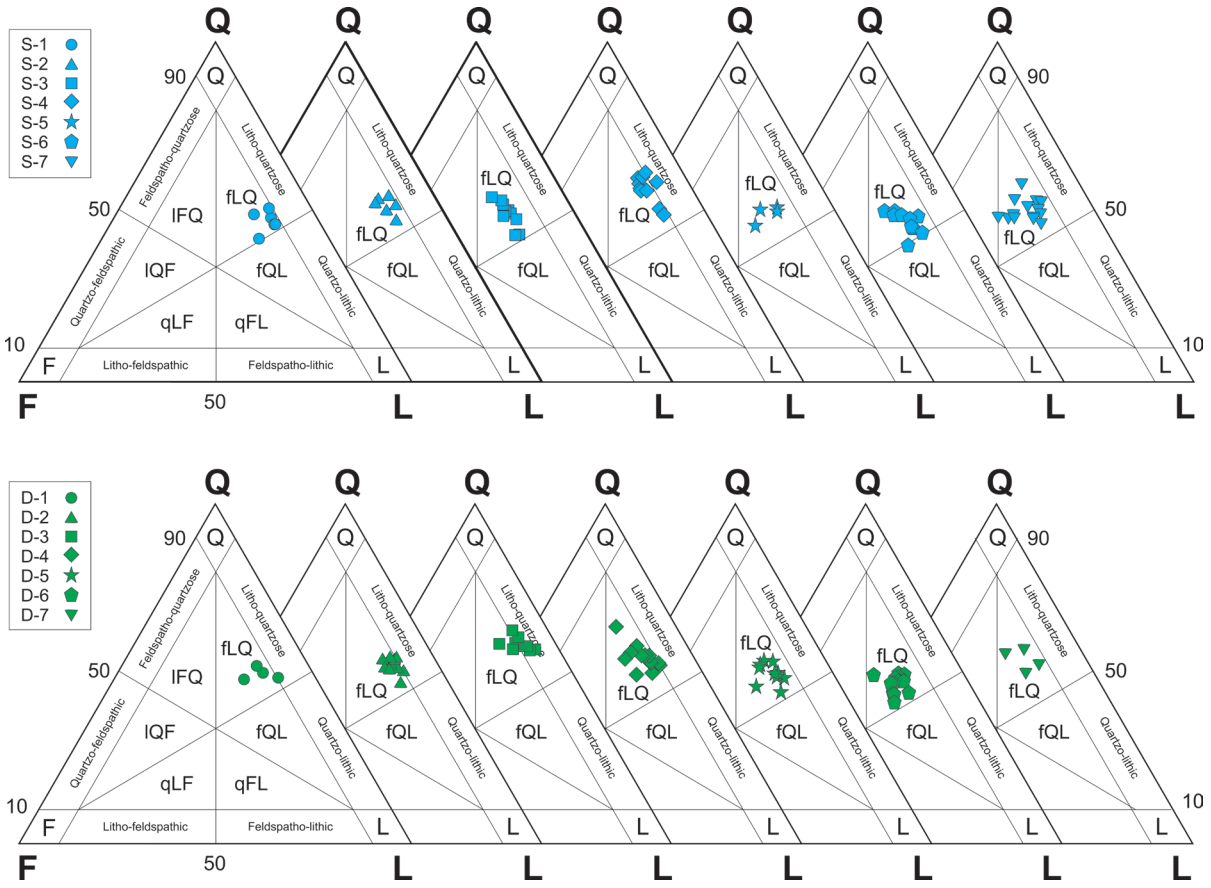

Fig. 6. QFL diagrams for the Upper Miocene sandstones from exploration wells of the Sava (S1–S7) and Drava Depression (D1–D7) according to Garzanti (2016).

Table 2: Rock fragments' modal composition of the Upper Miocene sandstones from the exploration wells of the Sava (S1–S7) and Drava Depression (D1–D7) with minimal, average, and maximal values for the individual component (excluding polycrystalline quartz). Lm – metamorphic rocks; Lv – magmatic (igneous) rocks; Ls – sedimentary rocks.

Exploration Well (Nr. of Samples)	**Lm (%)**			**Lv (%)**			**Ls (%)**		
	Min	Average	Max	Min	Average	Max	Min	Average	Max
S1 (6)	23.2	26.3	39	6	9	11.3	52.5	64.6	70.7
S2 (6)	28.7	32.1	41.8	5.2	8.2	14.3	51	59.6	65.5
S3 (10)	11.6	22.6	29.7	4.9	10.1	13.1	58.7	67.3	77.7
S4 (11)	19.8	31.5	37.9	5.4	7.2	10.9	56.5	61.3	74
S5 (4)	24	29.1	33.6	8.2	8.9	10	57.5	62	67.7
S6 (10)	19.6	26.3	34.2	5.5	11.9	18.3	51.4	61.9	71.4
S7 (14)	14.9	28.4	42.9	6.3	12.4	22.1	43.2	59.2	74.8
D1 (4)	14	22.6	26.6	5.1	6.6	9.4	64.1	70.8	80.9
D2 (10)	21.9	26.5	34.8	2.4	5.9	12.5	61.6	67.6	75.2
D3 (11)	22.2	29.9	37.9	2.2	7.6	14.5	49.5	62.4	71.7
D4 (13)	16.5	24.4	32.8	4.5	7.7	12.5	54.7	67.9	78
D5 (10)	16.2	30.9	41.9	9.4	17.2	28.5	37.4	51.9	60.6
D6 (17)	24.3	33	37.9	6.4	11.6	16.2	46.8	55.4	63
D7 (4)	21.2	29.7	35.9	5.7	8.3	10.1	55.4	62	70.2

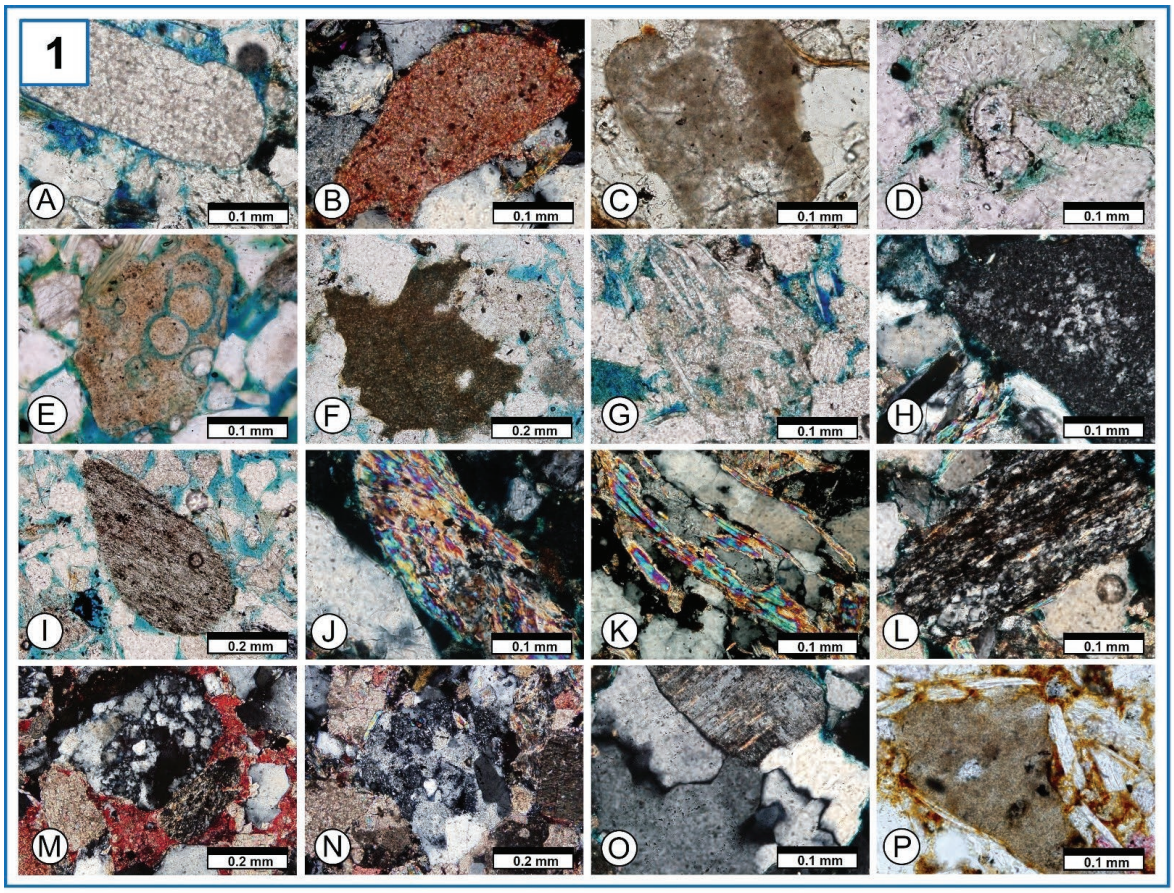
1
A
0.1 mm
B
0.1 mm
C
0.1 mm
D
0.1 mm
E
0.1 mm
F
0.2 mm
G
0.1 mm
H
0.1 mm
I
0.2 mm
J
0.1 mm
K
0.1 mm
L
0.1 mm
M
0.2 mm
N
0.2 mm
O
0.1 mm
P
0.1 mm

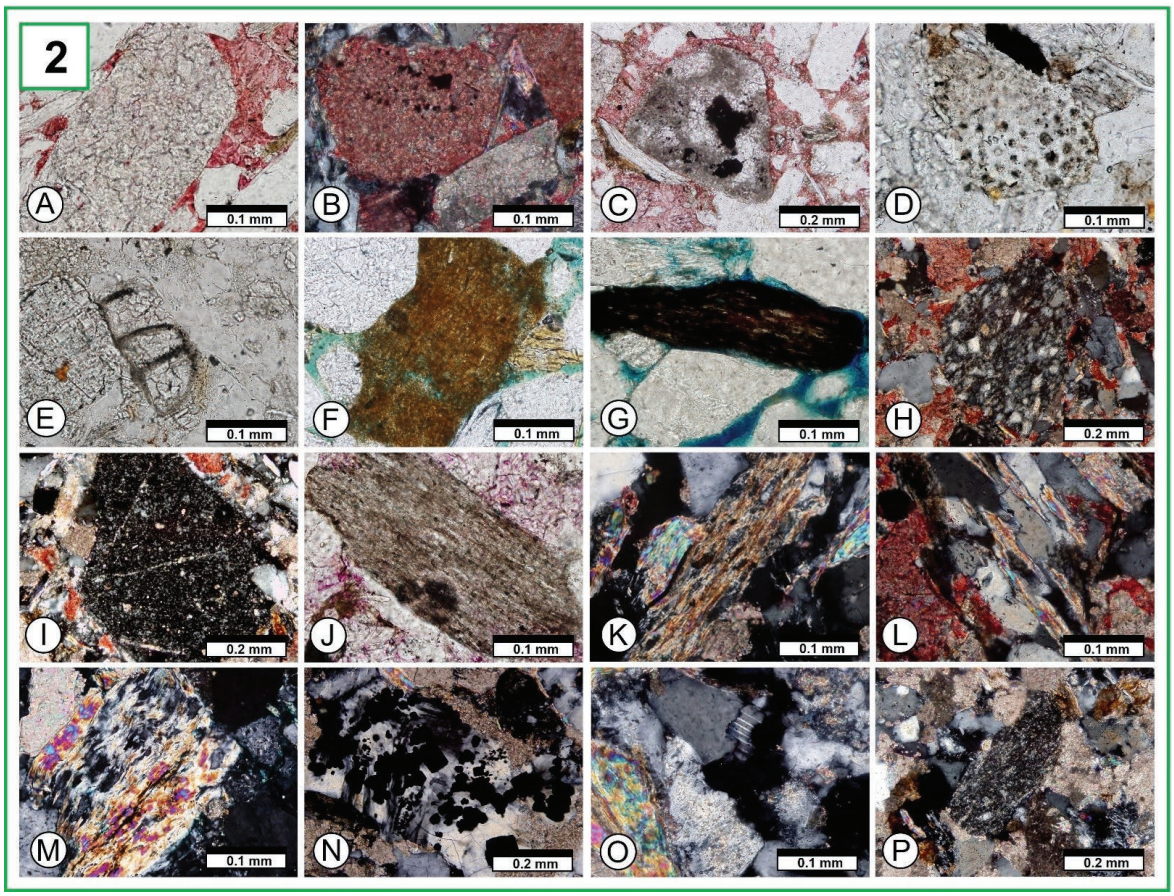
2
A
0.1 mm
B
0.1 mm
C
0.2 mm
D
0.1 mm
E
0.1 mm
F
0.1 mm
G
0.1 mm
H
0.2 mm
I
0.2 mm
J
0.1 mm
K
0.1 mm
L
0.1 mm
M
0.1 mm
N
0.2 mm
O
0.1 mm
P
0.2 mm

Fig. 7. Rock fragments in the Upper Miocene sandstones from the Sava Depression with sedimentary (A–H), metamorphic (I–M), and magmatic rock fragments (N–P). **(1): A** — Recrystallized dolomite (S4-4a, PPL); **B** — Recrystallized limestone (sparite) stained with Alizarin Red S (S7-3b, PPL); **C** — Limestone of packstone/grainstone type (S6-7, PPL); **D** — Recycled carbonatic bioclast (planktonic foraminifera shell) (S7-3b, PPL); **E** — Fossiliferous limestone (mudstone/wackestone; S5-1, PPL); **F** — Deformed unstable mudrock (marl rip-up clast; S6-2b, PPL); **G** — Siltstone (S4-3a, PPL); **H** — Chert (S1-3b, XPL); **I** — Metapellite/slate (S7-1, PPL); **J** — Fragment of mica schist under cross-polarized light (S5-2, XPL); **K** — Gneiss/schist (S7-2b, XPL); **L** — Microcrystalline mica schist (S1-3a, XPL); **M** — Quartzite (S1-1, XPL); **N** — Granitoid fragment (S7-5b, XPL); **O** — Granite (S4-5a, XPL); **P** — Altered volcanic rock (S6-1, PPL); and rock fragments in the Upper Miocene sandstones from the Drava Depression with sedimentary (A–I), metamorphic (J–N), and magmatic rock fragments (O & P). **(2): A** — Recrystallized dolomite (D5-2b, PPL); **B** — Recrystallized limestone (mudstone) stained with Alizarin Red S and dolomite (D7-2b, XPL); **C** — Limestone of grainstone type (D3-3, PPL); **D** — Recycled undetermined carbonatic bioclast (D4-2a, PPL); **E** — Fragment of carbonatic bioclast (bentic foraminifera shell; D5-1b, PPL); **F** — Deformed unstable rip-up clast of mudrock (claystone/marl; D2-1d, PPL); **G** — Mudrock rich in organic matter (shale; D7-1b, PPL); **H** — Siltstone under cross-polarized light (D4-3a, XPL); **I** — Chert (D3-1b, XPL); **J** — Metapellite/slate (D5-1a, PPL); **K** — Mica schist under cross-polarized light (D3-5a, XPL); **L** — Gneiss/mica schist (D7-2b, XPL); **M** — Fragment of mica schist (D2-3c, XPL); **N** — Quartzite with euhedral pyrite minerals (D4-5a, XPL); **O** — Granitoid rock fragment (D3-5b, XPL); **P** — Altered volcanoclastic rock (tuff; D2-3d, XPL). PPL = plane-polarized light, XPL = cross-polarized light. Photo: M. Matošević

have provenance mainly from carbonate, followed by low to medium-grade metamorphic and, to a lesser extent, granitoid rocks.

Detected small-scale originals of source rocks point toward recycled carbonate-clastic, axial belt metamorphic complex, and continental-block orogenic provenance (Garzanti 2016). Based on the QFL or QtFL modal compositions, according to Dickinson (1985) and Weltje (2006), the analyzed sandstones correspond to the tectonic setting of recycled orogen (subduction complex or fold-thrust belt; Fig. 10). This complex tectonic setting is the result of collisional processes that put together different tectonic units of the Alpine–Carpathian–Dinaridic orogenic system, including the basement of the PBS, which all represent potential source areas of the material in the Upper Miocene sandstones of the NCB. Furthermore, the tectonic units of Schmid et al. (2008, 2020) and the geological map of Europe by Asch (2003) were used to describe the regional geological situation (Fig. 1). The Southern Alps are mainly composed of Mesozoic carbonates, while the Eastern Alps and the Western Carpathians (ALCAPA mega-unit) are comprised of both Mesozoic carbonates and Proterozoic to Paleozoic low to medium-grade metamorphic rocks, with Paleozoic granitoids mainly confined to the Western Carpathians. Similarly, the Tisza mega-unit is predominantly composed of Paleozoic low to medium-grade metamorphic rocks and granitoids, with Upper Paleozoic and Mesozoic siliciclastic and carbonate sedimentary rocks. The Eastern and Southern Carpathians (Dacia mega-unit) are comprised of both Paleozoic medium to high-grade metamorphic rocks and Mesozoic ophiolitic rocks. At the same time, the Dinarides are mainly composed of Mesozoic carbonates (High Karst Unit and Dalmatian zone), partially metamorphosed Paleozoic siliciclastic rocks, and Mesozoic ophiolites (Pre-Karst Unit and Adria-derived nappes with Western Vardar Ophiolitic Unit). The innermost unit of the Dinarides is the Sava Zone, which is composed of various igneous, metamorphic, and sedimentary rocks of the Late Cretaceous. Additionally, various Mesozoic and younger siliciclastic flysch basins, as well as younger granitoid intrusions, volcanic rocks, volcaniclastics, and sedimentary rocks of the Late Cretaceous, Paleogene, and Neogene ages can be detected in different tectonic units in this region.

Parts of the PBS basement outcropping on the surface in the NCB today (e.g., Kalnik, Medvednica, Moslavačka Gora, Slavonian Mts.; e.g., Pamić & Lanphere 1991; Horvat et al. 2018; Starijaš et al. 2010; Biševac et al. 2010, 2011; Balen & Petrinec 2011; Balen et al. 2013, 2020; Belak et al. 2022; Schneider et al. 2022) or found deep in exploration wells in the depressions inside the NCB (e.g., Pamić 1986, 1999; Matošević et al. 2015; Matošević & Šuica 2017; Šuica et al. 2022a, b) also include the aforementioned types of rocks and belong to different tectonic units. They mostly incorporate tectonized magmatic, metamorphic, and sedimentary rocks belonging to the Tisza mega-unit, as well as the Sava zone and the Adria-derived nappes with Western Vardar Ophiolitic Unit of the Dinarides.

The massive inflow of detritus into the Lake Pannon during the Late Miocene (Bérczi et al. 1988; Juhász 1994; Magyar et al. 2013; Pavelić & Kovačić 2018; Anđelković & Radivojević 2021) produced considerable thicknesses of the sediments in the SD and DD (Ivković et al. 2000; Saftić et al. 2003; Kovačić et al. 2004; Kovačić & Grizelj 2006; Pavelić & Kovačić 2018; Malvić & Velić 2011). It is thus not likely that local parts of the NCB basement, with their relatively small volumes, served as the main sources of the material. Some islands within the lake and peninsulas that surrounded it at some point could have contributed to a smaller amount of the detritus (Bérczi 1988; Kovačić & Grizelj 2006; Sztanó et al. 2015). It is, however, not likely that these sources contributed greater amounts of detritus, since the lake reached its largest extension around 10.5 Ma (Magyar et al. 1999). Moreover, due to a high rate of subsidence of the basin and wet climate, great water depths developed (of up to 1000 m locally) leaving all the islands under water (Pogácsás 1984; Sztanó et al. 2013; Balázs et al. 2018). Finally, the Upper Miocene sediments cover some parts of the mountains in the NCB today and therefore signal their major uplift after the Late Miocene, i.e., during the later compressional phase of the basin evolution (e.g., Pavelić 2001; Tomljenović & Csontos 2001; Márton et al. 2002; Pavelić & Kovačić 2018).

The Lower and Middle Miocene rocks stratigraphically underlying the Upper Miocene sediments in northern Croatia include different types of sediments deposited in freshwater and marine environments, including fossiliferous carbonates and different types of siliciclastic sediments, as well as volcanic and volcaniclastic rocks (Tadej 2011; Kovačić et al. 2011; Matošević et al. 2015, 2019a; Pavelić & Kovačić 2018; Hernitz Kučenjak et al. 2018; Avanić et al. 2018, 2021; Brlek et al. 2020, 2023; Grizelj et al. 2020, 2023; Bigunac 2022; Kopecká et al. 2022; Premec Fućek et al. 2022; Sremac et al. 2022). Similar types of Lower and Middle Miocene rocks were also found in other basins of the PBS (cf. Rybár et al. 2016, 2019; Sant et al. 2020; Nyíri et al. 2021; Bordy & Sztanó 2021; Csibri et al. 2022). As a consequence, the possible local origin of some of the carbonatic fragments (e.g., micritic limestones and recycled carbonate bioclasts) or volcanic/volcaniclastic rocks in the Upper Miocene sandstones, which were possibly eroded from the underlying Lower and Middle Miocene rocks in the Late Miocene, cannot be completely ruled out. The same applies to siliciclastic sediments (e.g., mudrocks in the form of intrabasinal rip-up clasts) that could have been delivered from different parts of the PBS into the depressions and be partly of the same Late Miocene age. Nevertheless, a large share of fragments of carbonates in the sandstones does not bear any physical (textural) resemblance to those of the Early and Middle Miocene. They are principally non-fossiliferous and largely recrystallized. Even carbonatic bioclasts are found extremely rarely in the samples.

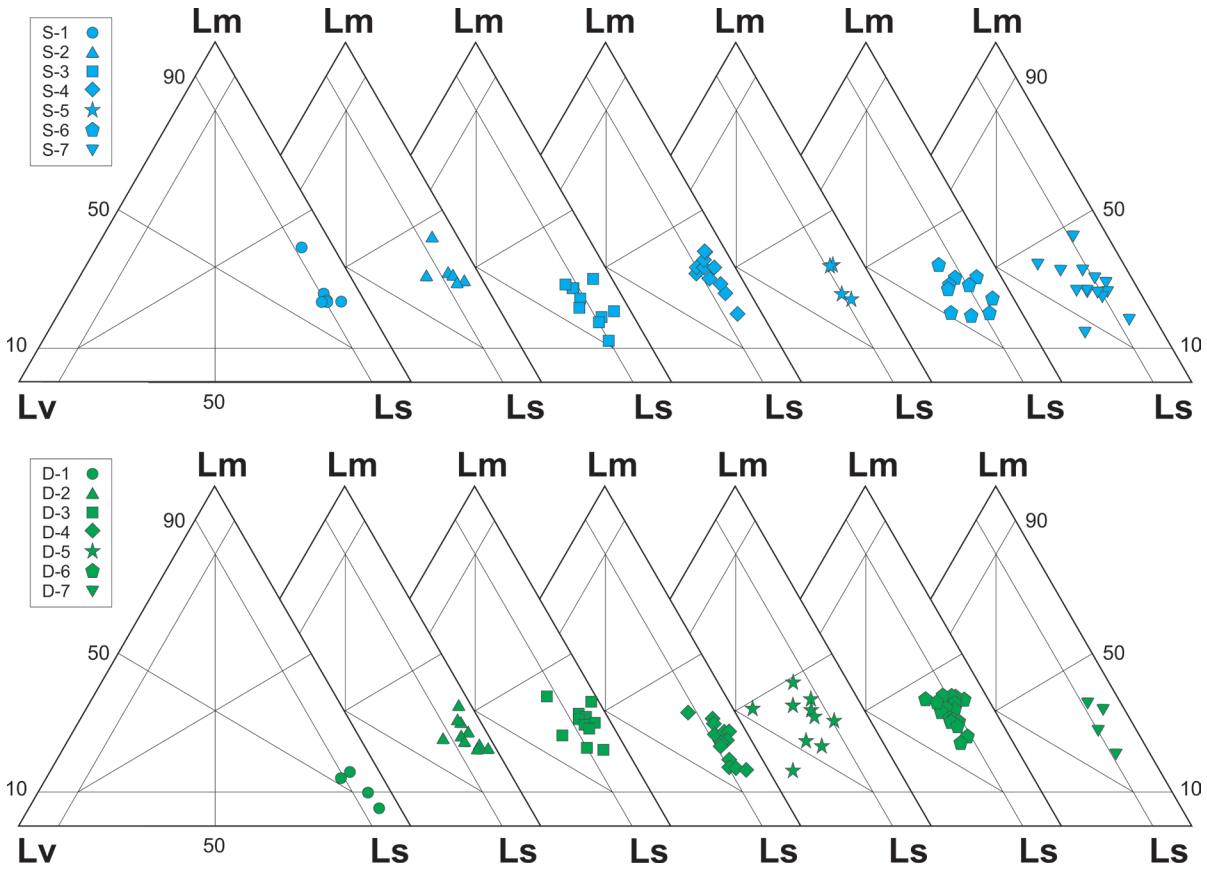

Fig. 8. LmLvLs diagrams of the Upper Miocene sandstones from exploration wells of the Sava (S1–S7) and Drava Depression (D1–D7) according to Garzanti (2019).

Fig. 9. Heavy mineral association in the Upper Miocene sandstones from the Sava Depression. **(1): A** — Garnet with inclusions and mechanical fractures surrounded by calcite cement (S1-1, PPL); **B** — Skeletal garnet (S1-3a, PPL); **C** — Rounded triangular cross-section of color-zoned tourmaline with irregular fractures (S7-3a, PPL); **D** — Tourmaline under cross-polarized light (S3-4b, XPL); **E** — Subhedral rutile (S2-2a, PPL); **F** — Epidote (S6-7, PPL); **G** — Clinozoisite (S5-1, XPL); **H** — Staurolite with inclusions (S5-1, PPL); **I** — Fractured zircon with inclusions under cross-polarized light (S7-3b, XPL); and heavy mineral association in the Upper Miocene sandstones from the Drava Depression. **(2): A** — Garnet within calcite-filled intergranular space (D4-4a, PPL); **B** — Etched garnet due to dissolution (D6-4b, PPL); **C** — Fractured skeletal garnet (D3-5c, PPL); **D** — Fractured and partly dissolved tourmaline (D3-1b, PPL); **E** — Trigonal cross-section of tourmaline under cross-polarized light (D4-2b, XPL); **F** — Fractured rutile under cross-polarized light (D2-3b, XPL); **G** — Prismatic apatite (D5-3, PPL); **H** — Staurolite (D6-5, XPL); **I** — Small zircon crystal with inclusions (D4-1c, PPL). PPL = plane-polarized light, XPL = cross-polarized light. Photo: M. Matošević

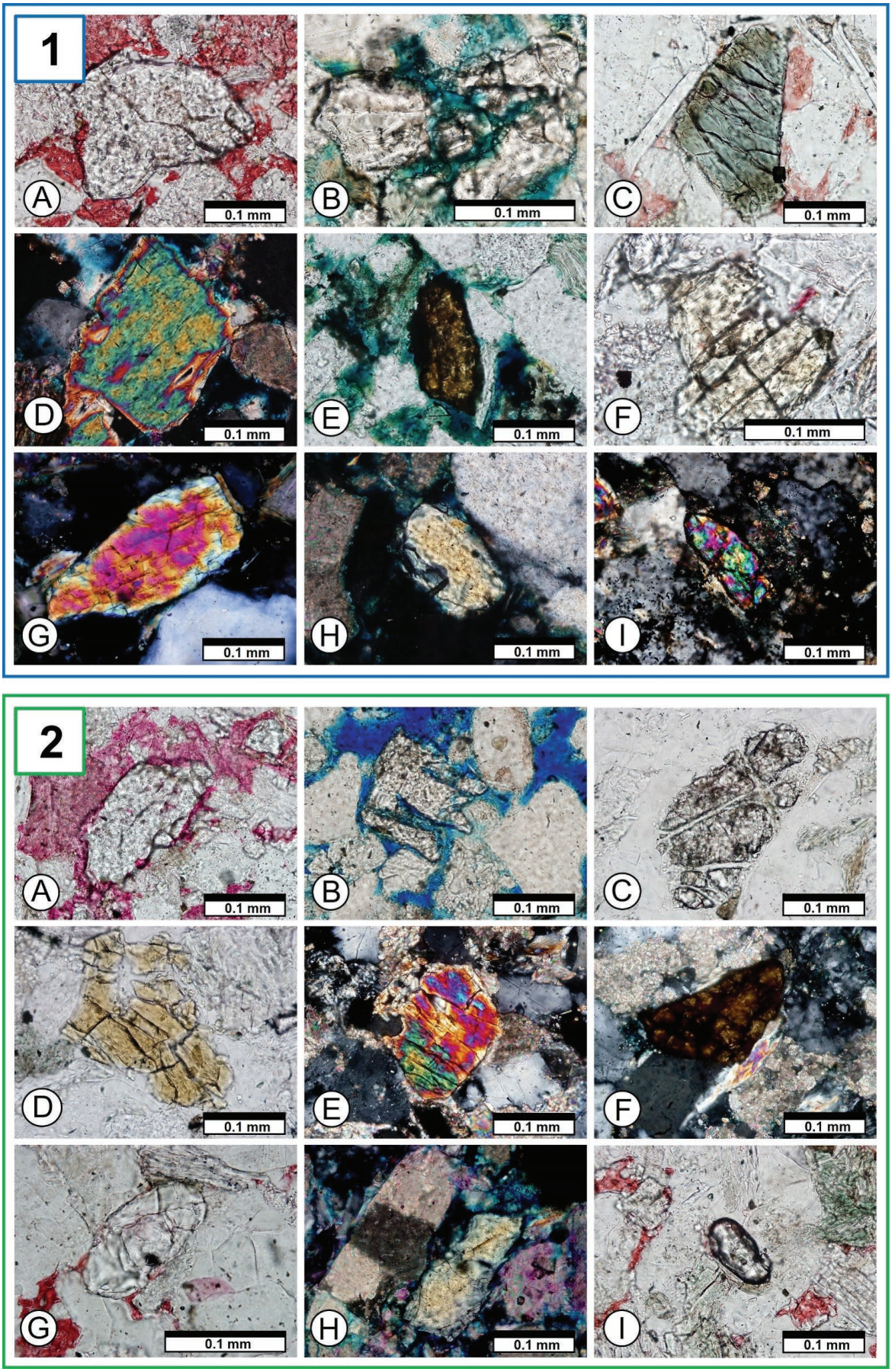
1
A
0.1 mm
B
0.1 mm
C
0.1 mm
D
0.1 mm
E
0.1 mm
F
0.1 mm
G
0.1 mm
H
0.1 mm
I
0.1 mm
2
A
0.1 mm
B
0.1 mm
C
0.1 mm
D
0.1 mm
E
0.1 mm
F
0.1 mm
G
0.1 mm
H
0.1 mm
I
0.1 mm

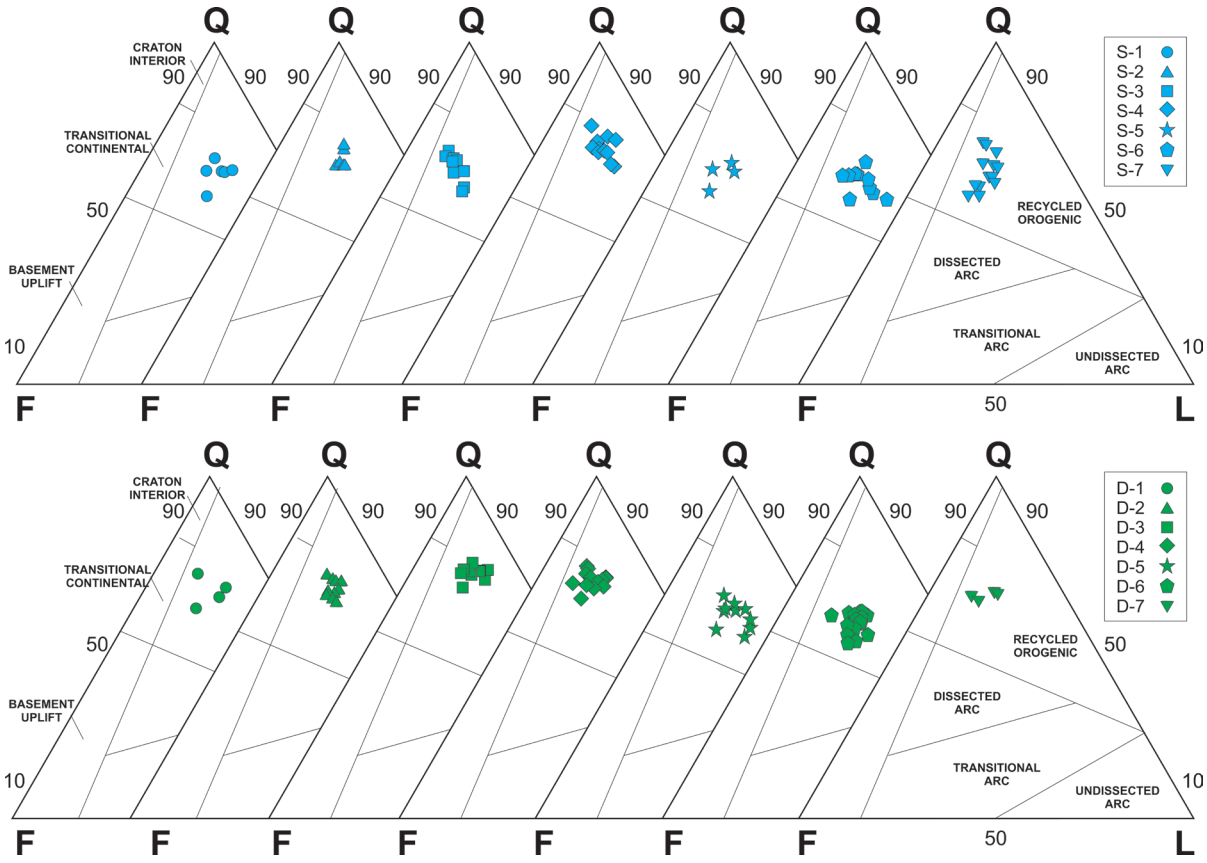

Fig. 10. QFL of the Upper Miocene sandstones from exploration wells of the Sava (S1–S7) and Drava Depression (D1–D7) showing their tectonic setting diagrams according to Dickinson (1985).

It is therefore possible to conclude that the fragments of carbonates correspond rather to those of the Paleozoic and Mesozoic age found in the surrounding area of the NCB and the PBS as a whole.

Furthermore, fragments of mudrocks, on average, form less than 0.7 %, while extrusive (volcanic) rocks form less than 0.3 % in the total modal composition. They are, in comparison to other rock fragments, insignificant for determining and interpreting main sources. According to von Eynatten (2003) and his modified conceptual model of the petrographic data based on Weltje et al. (1998), the weathering index for the Upper Miocene sandstones in the SD and DD corresponds to the field value '0' and indicates the early stages of weathering of plutonic and metamorphic/sedimentary source rocks in the high mountain relief area.

Earlier studies have shown that accumulated sediments in the PBS had mostly been eroded from the Eastern Alps and Carpathians between the Late Miocene (ca. 11–10 Ma) and Late Pliocene (Šćavničar 1979; Kuhlemann et al. 2002; Kovačić et al. 2004; Kovačić & Grizelj 2006; Magyar et al. 2013; Sebe et al. 2020). Nevertheless, it is often difficult to distinguish the Alpine and Carpathian sediment provenance, since they share a similar evolution history with similar bedrock composition (Arató et al. 2021). Since the Upper Miocene sandstones of the SD and DD do not contain any significant amounts of mafic and ultramafic rocks or radiolarites, nor any heavy minerals derived from these rocks (e.g., chrome spinel), the Dinarides, as well as the Southern and the Eastern Carpathians can be ruled out as main source areas (cf. Lužar-Oberiter et al. 2009, 2012; Ustaszewski et al. 2009, 2010). The exclusively Western Carpathian provenance would have resulted in a larger content of volcanic or volcaniclastic material (e.g., Seghedi & Downes 2011). Based on the previously mentioned lithic fragments determined in the sandstones, the Eastern Alps are proposed as the most probable major source area. Even studies of the present-day Drava and Mur River sediments, those sourced in the Eastern Alps with dominantly metamorphic lithologies, show similarities in the HM composition with the Upper Miocene sandstones from the SD and DD, with garnet as the major component, followed by epidote, amphibole, rutile, apatite, tourmaline, and titanite (Arató et al. 2021).

Progradation of the Upper Miocene sandstones' clinoforms from seismic profiles indicates high material inflow from N/NW and W directions into the SD and DD (Ivković et al. 2000; Saftić et al. 2003; Magyar et al. 2013; Špelić et al. 2019; Sebe et al. 2020). The same general directions were detected on the surface in the NCB (Kovačić & Grizelj 2006; Kovačić

et al. 2011). As inferred from the seismic data, parts of the DD depositional system are also locally characterized by sets of clinoform sediments with shelf-margin slope progradation from a N/NE towards S/SW direction. Similar findings in the Bjelovar sub-depression (Fig. 3) were recently demonstrated by Ružić (2021). Altogether, these findings point towards the Alps (Eastern Alps and potentially Southern Alps) as major source areas of the Upper Miocene sandstones, with a minor addition from the Carpathians (Western Carpathians and potentially Eastern Carpathians; Šćavničar 1979; Kovačić & Grizelj 2006; Kovačić et al. 2011; Magyar et al. 2013; Sztanó et al. 2013).

Additionally, there is no progradation of the sandstones' clinoforms observed from seismic profiles indicating main material inflow from S, SW, or SE directions into the SD and DD. Compositional equivalence, which was detected by petrographic analyses of the samples and paleotransport of the sandstones, implies that the two depressions were connected in the Late Miocene with no significant topographical obstacles for the inflow of the sandy detritus. This additionally supports the concept that the main uplift of the mountains in the NCB occurred during the Pliocene and Quaternary (Prelogović et al. 1998; Tomljenović & Csontos 2001; Pavelić 2001; Márton et al. 2002; Saftić et al. 2003; Pavelić & Kovačić 2018; Kurečić et al. 2021).

Almost all trends of relative changes in the sandstones' modal composition with the change of geographic position and depth are correspondent between the two depressions. They can be associated with characteristics and variations of the exhumation in the source area – in the form of potential primary erosion of covering sedimentary (carbonate) rocks and subsequent erosion of underlying metamorphic and magmatic (plutonic) rocks. This is indicated by the decrease of L and Lt values, supported by the decrease of Ls values, from the W/NW to the E/SE in both depressions, i.e., in the direction of the progradation of the sandstones. The same assumption is indicated by the increase of Lv and Lm values, supported by the increase of F values, from the W/NW to the E/SE, but also by the decrease of L and F values with depth. The observed trends could additionally be caused by the mixing of detritus before the final influx in the basin (e.g., a possible admixture of material from local islands and peninsulas or other rivers and tributaries from the northern and north-eastern parts of the PBS, such as the paleo-Danube and paleo-Tisza; e.g., Magyar et al. 2013). Further causes could also embrace weathering and alteration processes (including dissolution of carbonate rock fragments with time and length of the transport from source to sink), as well as the consequences of diagenetic processes within the basin (including stronger or weaker resistance of some grains to burial depth). The higher increase of Lv in D5 could indicate an increased inflow of plutonic (granitoid) detritus from other, possibly local source(s) or a possible existence of a minor geographic (topographical) barrier for the main inflow of detritus in this area (e.g., an island or an underwater elevation of the lake bottom). Changes in Ls with depth are primarily the result of diagenesis since they strongly depend on deformation, alteration, and dissolution during the burial. The same applies to the HM component – a significant decrease or complete absence of some of the minerals (e.g., epidote, clinozoisite, zoisite, staurolite, amphibole) in deeper intervals of the wells (generally deeper than 1000 m) is a direct consequence of their dissolution with depth, i.e., instability with increasing temperature, pressure, and interaction with pore fluids (Pettijohn 1957; Šćavničar 1979; Morton & Hallsworth 2007; Andò et al. 2012; Garzanti 2016). Some of the grains (e.g., F, Lv, and Lm, including their sub-groups) have been better preserved with depth in the DD than in the SD. The prevention of deformation and chemical alterations of the grains is a consequence of early carbonate cement precipitation in intergranular space in deeper parts of the DD. Similarly, changes in Q values with depth are largely the result of diagenesis, since quartz is more resistant to burial processes than other grains. Seeing that the sandstones from both depressions are exclusively very fine and fine-grained, it can be assumed that the grain size does not play a significant role in the distribution of trends of individual components. The changes in the HM share in relation to changes in the M share strongly support the theory of the influence of hydraulic sorting on the deposition of grains of the same provenance (Cascalho & Fradique 2007; Kompar 2007; Garzanti et al. 2008; Garzanti 2016).

Additionally, the NCB Upper Miocene sandstones largely differ from those from the Lower and Middle Miocene, which are subordinate oil and gas reservoirs in the area (Lučić et al. 2001; Saftić et al. 2003; Pavelić & Kovačić 2018). The sandstones from the two depressions are fine-grained, generally well- to moderately well-sorted, and texturally mature, in accordance with the results of previous studies (Kovačić et al. 2004, 2011; Kovačič & Grizelj 2006). They contain fragments of magmatic, metamorphic, and sedimentary rocks, including fragments of extrabasinal carbonates from further regional sources. The Lower and Middle Miocene sandstones are, by contrast, principally of coarser grain sizes, poorly-sorted, and texturally less mature. They were formed during the syn-rift phase of the PBS development and are frequently interbedded with breccias and conglomerates generated along normal faults associated with the initial rifting of the NCB (Pavelić et al. 1998; Saftić et al. 2003; Pavelić 2005; Matošević et al. 2015; Brlek et al. 2016; Pavelić & Kovačić 2018; Bigunac 2022). They are intermittently interbedded with volcaniclastic sediments and mudrocks (e.g., fossiliferous marls) associated with marine transgressions occurring during the existence of the Central Paratethys (Matošević et al. 2019a; Brlek et al. 2020, 2023; Marković et al. 2021; Grizelj et al. 2020, 2023; Premec Fućek et al. 2022; Sremac et al. 2022). As can be observed from seismic profiles, the paleo-transport of their detritus is from locally uplifted parts of the NCB basement with no preferable main transport directions, primarily perpendicular to the normal faults. The Lower and Middle Miocene sandstones form facies of alluvial fans and related fluvial and deltaic environments, with detritus being further transported into deeper parts of the depressions (Tadej 2011;

Pavelić & Kovačić 2018; Bigunac 2022). Aside from a much larger ratio of fragments of extrusive volcanic and volcaniclastic rock, they also include a much larger ratio of intrabasinal carbonatic rock fragments and abundant and diverse quantities of carbonate bioclasts (this applies especially to the Middle Miocene sandstones formed in marine environments; e.g., Brlek et al. 2016, 2023; Kovačić et al. 2011; Matošević et al. 2019a; Sremac et al. 2022; Premec Fućek et al. 2022; Grizelj et al. 2023). The findings of this study demonstrate that this is atypical for the Upper Miocene sandstones.

Conclusions

For the most part, the Upper Miocene sandstones from the SD and the DD in the NCB correspond to feldspatho–litho–quartzose sandstones and are interpreted to have been derived from a provenance area of a recycled orogen. Sandstones' modal compositions and detailed analyses of rock fragments and heavy minerals suggest an equivalent external source terrain without major local influences – parent rocks consist of carbonates, metamorphic rocks, and plutonic rocks, mainly of the Alpine–Carpathian fold belt (ALCAPA tectonic mega-unit). The uniform composition of the sandstones from both depressions suggests time-identical processes of source rock erosion, sandy material transport, and deposition, mainly as a relatively fast and massive inflow into the basin during the Late Miocene. Both depressions show an increase in the F, Lm, and Lv components, and a decrease in the Q, L, Lt, and Ls components from the W/NW towards the E/SE. These changes in the sandstones' composition reflect a combination of changes in the source area (erosion of parent rocks), alterations during transport, and mixing of the detrital material prior to deposition. An increase in the Q, Qp, and Lt components, as well as a decrease in F, K+P, L, Lm, TQM, Ls, Lncarb, and HM with depth was noticed in both depressions. In general, these changes in sandstone composition reflect diagenetic factors, such as the stability or instability of individual components to post-depositional alteration. Diagenetic alteration can be explained by compaction, the progressive increase of temperature and pressure with burial depth, and the presence of pore fluids. The Upper Miocene sandstones from the NCB differ in terms of their texture and composition from the Lower and the Middle Miocene sandstones in this area, which are of more local provenance. The results of the study show that no major morphological barriers were present between the SD and DD that could have obstructed the inflow of detrital material via rivers and deltas into the Lake Pannon. And so, the main uplift of the mountains in the NCB is inferred to have taken place after the Upper Miocene, which is consistent with previous studies.

Acknowledgements: The PhD scholarship of Mario Matošević is financed by the Faculty of Mining, Geology, and Petroleum Engineering, University of Zagreb. The research is a part of the SEDBAS project financed by the Croatian Science Foundation (IP-2019-04-7042). We acknowledge INA – Industrija nafte d.d. for support in conducting this research. We would like to thank Ljiljana Kirin for help with sample preparations, Gabrijela Pecimotika for paleontological analyses, and Neven Šuica for help with graphic design. The authors would also like to thank the reviewers, Katarína Šarinová and Róbert Arató, for their constructive comments and suggestions which improved the manuscript.

References

Alcalde J., Heinemann N., Mabon L., Worden R.H., De Coninck H., Robertson H., Maver M., Ghanbari S., Swennenhuis F., Mann I., Walker T., Gomersal S., Bond C.E., Allen M.J., Haszeldine R.S., James A., Mackay E.J., Brownsort P.A., Faulker D.R. & Murphy S. 2019: Acorn: Developing full-chain industrial carbon capture and storage in a resource- and infrastructure-rich hydrocarbon province. *Journal of Cleaner Production* 233, 963–971. https://doi.org/10.1016/j.jclepro.2019.06.087

Anđelković F. & Radivojević D. 2021: The Serbian Lake Pannon formations – their significance and interregional correlation. *Geološki anali Balkanskog poluostrva* 82, 43–67. https://doi.org/10.2298/GABP210420007A

Andò S., Garzanti E., Padoan M. & Limonta M. 2012: Corrosion of heavy minerals during weathering and diagenesis: A catalog for optical analysis. *Sedimentary Geology* 280, 165–178. https://doi.org/10.1016/j.sedgeo.2012.03.023

Arató R., Obbágy G., Dunkl I., Józsa S., Lünsdorf K., Szepesi J., Benkó Z. & Von Eynatten H. 2021: Multi-method comparison of modern river sediments in the Pannonian Basin System – A key step towards understanding the provenance of sedimentary basin-fill. *Global and Planetary Change* 199, 103446. https://doi.org/10.1016/j.gloplacha.2021.103446

Armstrong-Altrin J. & Verma S. 2005: Critical evaluation of six tectonic setting discrimination diagrams using geochemical data of Neogene sediments from known tectonic settings. *Sedimentary Geology* 177, 115–129. https://doi.org/10.1016/j.sedgeo.2005.02.004

Asch K. 2003: The 1:5 million international geological map of Europe and adjacent areas: development and implementation of a GIS-enabled concept. *Geological Yearbook*, SA 3, BGR, Hannover, ISBN 3510959035.

Augustsson C. 2021: Influencing factors on petrography interpretations in provenance research – a case study review. *Geosciences* 11, 205. https://doi.org/10.3390/geosciences11050205

Avanić R., Tibljaš D., Pavelić D. & Gverić Z. 2018: STOP 2: Zeolitized pyroclastics of the Donje jesenje. In: Tibljaš D., Horvat M., Tomašić N., Mileusnić M & Grizelj A. (Eds.): Conference Book, 9th Mid-European Clay Conference, Zagreb, September 17–21, 2018. *Croatian Geological Society, Croatian Geological Survey, Faculty of Mining, Geology and Petroleum Engineering & Faculty of Science – University of Zagreb*, 137–140.

Avanić R., Pavelić D., Pécskay Z., Miknić M., Tibljaš D. & Wacha L. 2021: Tidal deposits in the Early Miocene Central Paratethys: the Vučji Jarek and Čemernica members of the Macelj formation (NW Croatia). *Geologia Croatica* 74, 45–56. https://doi.org/10.4154/gc.2021.06

Balázs A. 2017: Dynamic model for the formation and evolution of the Pannonian Basin: The link between tectonics and sedimentation. *Utrecht Stud. Earth Sciences* 132, 153.

Balázs A., Matenco L., Magyar I., Horváth F. & Cloetingh S. 2016: The link between tectonics and sedimentation in back-arc basins: New genetic constraints from the analysis of the Pannonian Basin. *Tectonics* 35, 1526–1559. https://doi.org/10.1002/2015TC004109

Balázs A., Magyar I., Matenco L., Sztanó O., Tőkés L. & Horváth F. 2018: Morphology of a large paleo-lake: Analysis of compaction in the Miocene–Quaternary Pannonian Basin. *Global and Planetary Change* 171, 134–147. https://doi.org/10.1016/j.gloplacha.2017.10.012

Balen D. & Petrinec Z. 2011: Contrasting tourmaline type from peraluminous grnaites: A case study from Moslavačka Gora (Croatia). *Mineralogy and Petrology* 102, 117–134. https://doi.org/10.1007/s00710-011-0164-8

Balen D., Horváth P., Finger F. & Starijaš B. 2013: Phase equilibrium, geothermobarometric and xenotime age dating constraints on the Alpine metamorphism recorded in chloritoid schist from the southern part of the Tisia Mega-Unit (Slavonian Mts., NE Croatia). *International journal of earth science* 102, 1091–1109. https://doi.org/10.1007/s00531-012-0850-8

Balen D., Schneider P., Massonne H.J., Opitz J., Luptáková J., Putiš M. & Petrinec Z. 2020: The Late Cretaceous A-type alkali-feldspar granite from Mt. Požeška Gora (N Croatia): Potential marker of fast magma ascent in the Europe-Adria suture zone. *Geologica Carpathica* 71, 361–381. https://doi.org/10.31577/GeolCarp.71.4.5

Barić G., Ivković Ž. & Perica R. 2000: The Miocene petroleum system of the Sava Depression, Croatia. *Petroleum Geoscience* 6, 165–173. https://doi.org/10.1144/petgeo.6.2.165

Belak M., Slovenec D., Kolar-Jurkovšek T., Garašić V., Pécskay Z., Tibljaš D. & Mišur I. 2022: Low-grade metamorphic rocks of the Tethys subduction-collision zone in the Medvednica Mt. (NW Croatia). *Geologica Carpathica* 73, 207–229. https://doi.org/10.31577/GeolCarp.73.3.3

Bérczi I. 1988: Preliminary sedimentological investigations of a characteristic Neogene depression in the Great Hungarian plain (SE Hungary). In: Royden L.H. & Horváth F. (Eds.): The Pannonian Basin – A study in basin evolution. *AAPG Memoir* 45, 107–116.

Bérczi I., Hámor G., Jámbor Á. & Szentgyörgyi K. 1988: Neogene sedimentation in Hungary. In: Royden L.H. & Horváth F. (Eds.): The Pannonian Basin – A study in basin evolution. *AAPG Memoir* 45, 57–67.

Bhatia M. 1983: Plate tectonics and geochemical composition of sandstones. *The Journal of Geology* 91, 611–627.

Bigunac D. 2022: Depositional environments and subsurface settings of the Lower Miocene sediments in the Slavonia-Srijem, Drava and Sava Depressions. *Dissertation, Faculty of mining, geology and petroleum engineering, University of Zagreb*.

Biševac V., Balogh K., Balen D. & Tibljaš D. 2010: Eoalpine (Cretaceous) very low-to low-grade metamorphism recorded on the illite-muscovite-rich fraction of metasediments from South Tisia (eastern Mt Papuk, Croatia). *Geologica Carpathica* 61, 469–481. https://doi.org/10.2478/v10096-010-0029-9

Biševac V., Krenn E., Balen D., Finger F. & Balogh K. 2011: Petrographic, geochemical and geochronological investigation on granitic pebbles from Permotriassic metasediments of the Tisia terrain (eastern Papuk, Croatia). *Minerlaogy and Petrology* 102, 163–180. https://doi.org/10.1007/s00710-011-0175-5

Bordy E.M. & Sztanó O. 2021: Badenian (middle Miocene) continental paleoenvironment in the Novohrad–Nógrád Basin (Central Paratethys): a volcano-sedimentary record from the Páris-patak Valley in Hungary. *Földtani Közlöny* 151, 159–159. https://doi.org/10.23928/foldt.kozl.2021.151.2.159

Brlek M., Špišić M., Brčić V., Mišur I., Kurečić T., Miknić M., Avanić R., Vrsaljko D. & Slovenec D. 2016: Mid-Miocene (Badenian) transgression on Mesozoic basement rocks in the Mt. Medvednica area of northern Croatia. *Facies* 62, 1–21. https://doi.org/10.1007/s10347-016-0470-z

Brlek M., Kutterolf S., Gaynor S., Kuiper K., Belak M., Brčić V., Holcová K., Wang K.L., Bakrač K., Hajek-Tadesse V., Mišur I., Horvat M., Šuica S. & Schaltegger U. 2020: Miocene syn-rift evolution of the North Croatian Basin (Carpathian-Pannonian Region): new constraints from Mts. Kalnik and Požeška gora volcaniclastic record with regional implications. *International Journal of Earth Science* 109, 2775–2800. https://doi.org/10.1007/s00531-020-01927-4

Brlek M., Tapster S.R., Schindlbeck-Belo J., Gaynor S.P., Kutterolf S., Hauff F., Georgiev S.V., Trinajstić N., Šuica S., Brčić V., Wang K.L., Lee H.Y., Beier C., Abersteiner A.B., Mišur I., Peytcheva I., Kukoč D., Németh B., Trajanova M., Balen D., Guillong M., Szymanowski D. & Lukács R. 2023: Tracing widespread Early Miocene ignimbrite eruptions and petrogenesis at the onset of the Carpathian-Pannonian Region silicic volcanism. *Gondwana Research* 116, 40–60. https://doi.org/10.1016/j.gr.2022.12.015

Cascalho J. & Fradique C. 2007: The Sources and Hydraulic Sorting of Heavy Minerals on the Northern Portuguese Continental Margin. In: Mange M.A. & Wright D.T. (Eds.): Developments in Sedimentology. *Elsevier* 58, 75–112. https://doi.org/10.1016/S0070-4571(07)58003-9

Csibri T., Ruman A., Hudáčková N., Jamrich M., Sliva Ľ., Šarinová K. & Kováč M. 2022: Deltaic systems of the northern Vienna Basin: The lower-middle Miocene conglomerate bodies. *Geologica Carpathica* 73, 245–269. https://doi.org/10.31577/GeolCarp.73.3.5

Davies A. & Simmons M.D. 2021: Demand for 'advantaged' hydrocarbons during the 21st century energy transition. *Energy Reports* 7, 4483–4497. https://doi.org/10.1016/j.egyr.2021.07.013

Dickinson W.R. 1970: Interpreting detrital modes of graywacke and arkose. *Journal of Sedimentary Research* 40, 695–707. https://doi.org/10.1306/74D72018-2B21-11D7-8648000102C1865D

Dickinson W.R. 1985: Interpreting provenance relations from detrital modes of sandstones. In: Zuffa G.G. (Ed.): Provenance of arenites. *Reidel*, Dordrecht, *NATO ASI Series* 148, 333–361.

Dickinson W.R. & Suczek C.A. 1979: Plate tectonics and sandstone composition. *Beulletin of the AAPG* 63, 2164–2182.

Dickinson W.R., Beard L.S., Brakenridge G.R., Erjavec J.L., Ferguson R.C., Inman K.F., Knepp R.A., Lindberg F.A. & Ryberg P.T., 1983: Provenance of Noth American Phanerozoic sandstones in relation to tectonic setting. *GSA Bulletin* 94, 222–235. https://doi.org/10.1130/0016-7606(1983)94<222:PONAPS>2.0.CO;2

Dolton L.G. 2006: Pannonian Basin Province, Central Europe (Province 4808) – Petroleum geology, total petroleum systems, and petroleum resource assessment. *U.S. Geological Survey, Bulletin* 2204-B. https://doi.org/10.3133/b2204B

Ehrenberg S.N. 1990: Relationship between diagenesis and reservoir quality in sandstones of the Garn Formation, Haltenbanken, Mid-Norweigian continental shelf. *AAPG Bulletin* 74, 1538–1558. https://doi.org/10.1306/0C9B2515-1710-11D7-8645000102C1865D

Evamy B.D. & Shearman D.J. 1962: The application of chemical staining techniques to the study of diagenesis in limestones. *Proceedings of the Geological Society, London* 1599, 102.

Folk R.L. 1951: Stages of textural maturity in sedimentary rocks. *Journal of Sedimentary Research* 21, 127–130. https://doi.org/10.2110/jsr.21.127

Garzanti E. 2016: From static to dynamic provenance analysis – Sedimentary petrology upgraded. In: Caracciolo L., Garzanti E., Von Eynatten H. & Weltje G.J. (Eds.): Sediment generation and provenance: processes and pathways. *Sedimentary Geology* 336, 3–13. https://doi.org/10.1016/j.sedgeo.2015.07.010

Garzanti E. 2019: Petrographic classification of sand and sandstone. *Earth-Science Reviews* 192, 545–563. https://doi.org/10.1016/j.earscirev.2018.12.014

Garzanti E., Ando S. & Vezzoli G. 2008: Settling equivalence of detrital minerals and grain-size dependence of sediment composition. *Earth and Planetary Science Letters* 273, 138–151. https://doi.org/10.1016/j.epsl.2008.06.020

Gier S., Worden R.H., Johns W.D. & Kurzweil H. 2008: Diagenesis and reservoir quality of Miocene sandstones in the Vienna Basin, Austria. *Marine and Petroleum Geology* 25, 681–695. https://doi.org/10.1016/j.marpetgeo.2008.06.001

Grizelj A., Milošević M., Bakrač K., Galović I., Kurečić T., Hajek-Tadesse V., Avanić R., Miknić M., Horvat M., Čaić A. & Matošević M. 2020: Paleoecological and sedimentological characterization of Middle Miocene sediments from the Hrvatska Kostajnica area (Croatia). *Geologia Croatica* 73 153–175. https://doi.org/10.4154/gc.2020.15

Grizelj A., Milošević M., Miknić M., Hajek-Tadesse V., Bakrač K., Galović I., Badurina L., Kurečić T., Wacha L., Šegvić B., Matošević M., Čaić-Janković A. & Avanić R. 2023: Evidence of Early Sarmatian volcanism in the Hrvatsko Zagorje Basin, Croatia: Mineralogical, geochemical and biostratigraphic approaches. *Geologica Carpathica* 74, 59–82. https://doi.org/10.31577/GeolCarp.2023.02

Harzhauser M. & Mandic M. 2008: Neogene lake systems of the Central and South-Eastern Europe – faunal diversity, gradients and interrelations. *Palaeogeography, Palaeoclimatology, Palaeoecology* 260, 417–434. https://doi.org/10.1016/j.palaeo.2007.12.013

Harzhauser M. & Piller W.E. 2007: Benchmark data of a changing sea – palaeogeography, palaeobiogeography and events in the Central Paratethys during the Miocene. *Palaeogeography, Palaeoclimatology, Palaeoecology* 253, 8–31. https://doi.org/10.1016/j.palaeo.2007.03.031

Harzhauser M., Latal C. & Piller W. 2007: The stable isotope archive of Lake Pannon as a mirror of Late Miocene climate change. *Palaeogeography, Palaeoclimatology, Palaeoecology* 249, 335–350. https://doi.org/10.1016/j.palaeo.2007.02.006

Hernitz Kučenjak M., Premec Fućek V., Krizmanić K., Tadej J., Zlatar S. & Matošević M. 2018: Karpatian and Badenian transgressions in Croatian part of the Pannonian Basin System (biostratigraphy and palaeoenvironments). Forams 2018. *Temporary Abstract Collection*, Edinburgh, 273–274.

Hilgen F.J., Lourens L.J. & Van Dam J.A. 2012: The Neogene Period. In: Gradstein F.M., Ogg J.G., Schmitz M. & Ogg G. (Eds.): The Geologic Time Scale 2012. *Elsevier*, Amsterdam, 923–978. https://doi.org/10.1016/B978-0-444-59425-9.00029-9

Horvat M., Klötzli U., Jamičić D., Buda G., Klötzli E. & Hauzenberger C. 2018: Geochronology of granitoids from Psunj and Papuk Mts., Croatia. *Geochronometria* 45, 198–210. https://doi.org/10.1515/geochr-2015-0099

Horváth F. 1993: Towards a mechanical model for the formation of the Pannonian Basin. *Tectonophysics* 226, 333–357. https://doi.org/10.1016/0040-1951(93)90126-5

Horváth F. 1995: Phases of compression during the evolution of the Pannonian Basin and its bearing on hydrocarbon exploration. *Marine and Petroelum Geology* 12, 837–844. https://doi.org/10.1016/0264-8172(95)98851-U

Horváth F. & Royden L.H. 1981: Mechanism for formation of the intra-Carpathian basins: A review. *Earth Evolution Sciences* 1, 307–316.

Horváth F., Bada G., Szafián P., Tari G., Ádám A. & Cloetingh S. 2006: Formation and deformation of the Pannonian Basin: constrains from observational data. In: Gee D.G. & Stephenson R.A. (Eds.): European Lithosphere Dynamics. *Geological Society of London Memoirs* 32, 191–206. https://doi.org/10.1144/GSL.MEM.2006.032.01.11

Horváth F., Musitz B., Balázs A., Vegh A., Uhrin A., Nador A., Koroknai B., Pap N., Toth T. & Worum G. 2015: Evolution of the Pannonian basin and its geothermal resources. *Geothermics* 53, 328–352. https://doi.org/10.1016/j.geothermics.2014.07.009

Ibbeken H. & Schleyer R. 1991: Source and Sediment. *Springer*, Berlin, 1–286.

Ingersoll R.V., Bullard T.F., Ford R.L., Grimm J.P., Pickle J.D. & Sares S.W. 1984: The effect of grain size on detrital modes: a test of the Gazzi-Dickinson point-counting method. *Journal of Sedimentary Research* 54, 103–116. https://doi.org/10.1306/212F83B9-2B24-11D7-8648000102C1865D

Ivković Ž., Matej S. & Škoko M. 2000: Seismostratigraphic interpretation of Upper Miocene and Pliocene sediments of the Sava depression. In: Vlahović I. & Biondić R. (Eds.): *Second Croatian Geological Congress, Proceedings*, Zagreb, 219–222.

Jamičić D. 1983: Strukturni sklop metamorfnih stijena Krndije i južnih padina Papuka. *Geološki vjesnik* 36, 51–72.

Jerram D.A. 2001: Visual comparators for degree of grain-size sorting in two and three-dimensions. *Computers & Geosciences* 27, 485–492. https://doi.org/10.1016/S0098-3004(00)00077-7

Juhász Gy. 1991: Lithostratigraphical and sedimentological framework of the Pannonian (s.l.) sedimentary sequence in the Hungarian Plain (Alföld), Eastern Hungary. *Acta Geologica Hungarica* 34, 53–72.

Juhász Gy. 1994: Comparison of the sedimentary sequences in Late Neogene subbasins in the Pannonian Basin, Hungary [Magyarországi neogén medencerészek pannóniai s.l. üledéksorának összehasonlító elemzése]. *Földtani Közlöny* 124, 341–365.

Kolenković Močilac I., Cvetković M., Saftić B. & Rukavina D. 2022: Porosity and permeability model of a regional extending unit (Upper Miocene sandstones of the western part of Sava Depression, Croatia) based on vintage well data. *Energies* 15, 6066. https://doi.org/10.3390/en15166066

Kompar P.D. 2007: The entrainment, transport and sorting of heavy minerals by waves and currents. In: Mange M.A. & Wright D.T. (Eds.): *Developments in Sedimentology* 58, 3–48. https://doi.org/10.1016/S0070-4571(07)58001-5

Kopecká J., Holcová K., Brlek M., Scheiner F., Ackerman L., Rejšek J., Milovský R., Baranyi V., Gaynor S., Galović I., Brčić V., Belak M. & Bakrač K. 2022: A case study of paleoenvironmental interactions during the Miocene Climate Optimum in southwestern Paratethys. *Global and Planetary Change* 211, 103784. https://doi.org/10.1016/j.gloplacha.2022.103784

Kováč M., Nagymarosy A., Oszczypko N., Slaczka A., Csontos L., Marunteanu M., Matenco L. & Márton M. 1998: Palinspastic reconstruction of the Carpathian - Pannonian region during the Miocene. In: Rakús M. (Ed.): Geodynamic Development of the Western Carpathians. *Geol. Survey of Slovak Republic*, Bratislava, 189–217.

Kováč M., Márton E., Oszczypko N., Vojtko R., Hók J., Králiková S., Plašienka D., Klučiar T., Hudáčková N. & Oszczypko-Clowes M. 2017: Neogene palaeogeography and basin evolution of the Western Carpathians, Northern Pannonian domain and adjoining areas. *Global and Planetary Change* 155, 133–154. https://doi.org/10.1016/j.gloplacha.2017.07.004

Kováč M., Halásová E., Hudáčková N., Holcová K., Hyžný M., Jamrich M. & Ruman A. 2018: Towards better correlation of the Central Paratethys regional time scale with the standard geological time scale of the Miocene Epoch. *Geologica Carpathica* 69, 283–300. https://doi.org/10.1515/geoca-2018-0017

Kovačić M. & Grizelj A. 2006: Provenance of the Upper Miocene clastic material in the southwestern Pannonian Basin. *Geologica Carpathica* 57, 495–510.

Kovačić M., Zupanič J., Babić L., Vrsaljko D., Miknić M., Bakrač K., Hećimović I., Avanić R. & Brkić M. 2004: Lacustrine basin to delta evolution in the Zagorje Basin, a Pannonian sub-basin (Late Miocene: Pontian, NW Croatia). *Facies* 50, 19–33.

Kovačić M., Horvat M., Pikija M. & Slovenec D. 2011: Composition and provenance of Neogene sedimentary rocks of Dilj gora Mt. (south Pannonian Basin, Croatia). *Geologia Croatica* 64, 121–132. https://doi.org/10.4154/GC.2011.10

Krumbein W.C. & Sloss L.L.: 1963: Stratigraphy and sedimentation. *W.H. Freeman and Co.*, San Francisco, 1–660.

Kuhlemann J., Frisch W., Székely B., Dunkl, I. & Kázmér M. 2002: Post-collisional sediment budget history of the Alps: tectonic versus climatic control. *International Journal of Earth Sciences* 91, 818–837. https://doi.org/10.1007/s00531-002-0266-y

Kurečić T. 2017: Sedimentology and paleoecology of Pliocene Viviparus beds from the area of Vukomeričke gorice. *Dissertation, Faculty of Science, University of Zagreb.*

Kurečić T., Kovačić M. & Grizelj A. 2021: Mineral assemblage and provenance of the Pliocene Viviparus beds from the area of Vukomeričke Gorice (Central Croatia). *Geologia Croatica* 74, 253–271. https://doi.org/10.4154/gc.2021.16

Lawan A.Y., Worden R.H., Utley J.E.P. & Crowley S.F. 2021: Sedimentological and diagenetic controls on the reservoir quality of marginal marine sandstones buried to moderate depths and temperatures: Brent Province, UK North Sea. *Marine and Petroleum Geology* 128, 104993. https://doi.org/10.1016/j.marpetgeo.2021.104993

Lučić D., Saftić B., Krizmanić K., Prelogović E., Britvić V., Mesić I. & Tadej J. 2001: The Neogene evolution and hydrocarbon potential of the Pannonian Basin in Croatia. *Marine and Petroleum Geology* 18, 133–147. https://doi.org/10.1016/S0264-8172(00)00038-6

Lužar-Oberiter B., Mikes T., Von Eynatten H. & Babić L. 2009: Ophiolitic detritus in Cretaceous clastic formations of the Dinarides (NW Croatia): evidence from Cr-spinel chemistry. *International Journal of Earth Science* 98, 1097–1108. https://doi.org/10.1007/s00531-008-0306-3

Lužar-Oberiter B., Mikes T., Dunkl I., Babić L. & Von Eynatten H. 2012: Provenance of Cretaceous Synorogenic sediments from the NW Dinarides (Croatia). *Swiss Journal of Geosciences* 105, 377–399. https://doi.org/10.1007/s00015-012-0107-3

Magyar I. 2021: Chronostratigraphy of clinothem-filled non-marine basins: Dating the Pannonian Stage. *Global and Planetary Change* 205, 103609. https://doi.org/10.1016/j.gloplacha.2021.103609

Magyar I., Geary D.H. & Müller P. 1999: Paleogeographic evolution of the Late Miocene Lake Pannon in central Europe. *Palaeogeography, Palaeoclimatology, Palaeoecology* 147, 151–167. https://doi.org/10.1016/S0031-0182(98)00155-2

Magyar I., Radivojević D., Sztanó O., Synak R., Ujszászi K. & Pócsik M. 2013: Progradation of the paleo-Danube shelf margin across the Pannonian Basin during the Late Miocene and Early Pliocene. *Global and Planetary Change* 103, 168–173. https://doi.org/10.1016/j.gloplacha.2012.06.007

Malvić T. 2011: Geological maps of Neogene sediments in the Bjelovar Subdepression (northern Croatia). *Journal of Maps* 7, 304–317. https://doi.org/10.4113/jom.2011.1185

Malvić T. & Cvetković M. 2013: Lithostratigraphic units in the Drava Depression (Croatian and Hungarian parts) – a correlation. *Nafta* 64, 27–33.

Malvić T. & Velić J. 2011: Neogene tectonics in Croatian part of the Pannonian Basin and reflectance in hydrocarbon accumulations. In: Schattner U. (Ed.): New frontiers in tectonic research: At the midst of plate convergence. *Intech*, Rijeka, 215–238.

Mandic O., Kurečić T., Neubauer T.A. & Harzhauser M. 2015: Stratigraphic and palaeogeographic significance of lacustrine molluscs from the Pliocene Viviparus beds in Central Croatia. *Geologia Croatica* 68, 179–207. https://doi.org/10.4154/GC.2015.15

Marković F., Kuiper K., Ćorić S., Hajek-Tadesse V., Hernitz Kučenjak M., Bakrač K., Pezelj D. & Kovačić M. 2021: Middle Miocene marine flooding : new 40Ar/39Ar age constraints with integrated biostratigraphy on tuffs from the North Croatian Basin. *Geologia Croatica* 74, 237–252. https://doi.org/10.4154/gc.2021.18

Márton E., Pavelić D., Tomljenović B., Pamić J. & Márton P. 1999: First paleomagnetic results on Ternary rocks from the Slavonian Mountains in the Southern Pannonian Basin, Croatia. *Geologica Carpathica* 50, 273–279.

Márton E., Pavelić D., Tomljenović B., Avanić R., Pamić J. & Márton P. 2002: In the wake of a counterclockwise rotating Adriatic microplate: Neogene paleomagnetic results from northern Croatia. *International Journal of Earth Sciences* 91, 514–523. https://doi.org/10.1007/s00531-001-0249-4

Matenco L.C. & Radivojević D. 2012: On the formation and evolution of the Pannonian Basin: constraints derived from the structure of the junction area between the Carpathians and Dinarides. *Tectonics* 31. https://doi.org/10.1029/2012TC003206

Matošević M. & Šuica S. 2017: Microstructural characteristics of staurolite from mica schist of the Drava depression basement (Croatia). In: Gajović A., Weber I., Kovačević G., Čadež V., Šegota S., Peharec Štefanić P. & Vidoš A. (Eds.): 13th Multinational Congress on Microscopy: Book of abstracts, Rovinj, Croatia, September 24–29, 2017. *Ruđer Bošković Institute and Croatian Microscopy Society*, 520–521.

Matošević M., Slavković R. & Tomašić N. 2015: Occurrence of radiating Fe-oxides and Fe-oxyhydroxides crystal groups in the rocks of cores from the borehole Bunjani-59, Croatia. In: Ambriović Ristov A., Gajović A., Weber I. & Vidoš A. (Eds.): Proceedings of the 3rd Croatian Microscopy Congress with International Participation, Zadar, Croatia, April 26–29, 2015. *Ruđer Bošković Institute and Croatian Microscopy Society*, 83–84.

Matošević M., Hernitz Kučenjak M., Fuček V., Krizmanić K., Mikša G. & Troskot-Čorbić T. 2019a: The middle Badenian deep-marine sedimentation in the Central Paratethys: A case study of the Sava depression in the North Croatian Basin. In: Horvat M., Matoš B. & Wacha L. (Eds.): Proceedings of the 6th Croatian Geological Congress with International Participation. Zagreb, Croatia, October 9–12, 2019. *Croatian Geological Society*, 128–129.

Matošević M., Krizmanić K., Zlatar S., Hernitz Kučenjak M., Mikša G. & Pecimotika G. 2019b: Using ultraviolet light for fast sedimentological analysis and characterization of reservoir rocks: A case study of the Upper Miocene sediments from the Sava Depression, Croatia. Proceedings of the 34th IAS Meeting of Sedimentology. Rome, Italy, September 10–13, 2019. *The International Association of Sedimentologists and the Earth Science Department of Sapienza University of Roma.*

Matošević M., Pavelić D. & Kovačić M. 2019c: Petrography of the Upper Miocene sandstones from the Sava and Drava Depressions: Basis for understanding the provenance and diagenesis of the largest hydrocarbon reservoirs in the North Croatian Basin. In: Horvat M., Matoš B. & Wacha L. (Eds.): Proceedings of the 6th Croatian Geological Congress with International Participation. Zagreb, Croatia, October 9–12, 2019. *Croatian Geological Society*, 127–128.

Matošević M., Kovačić M. & Pavelić D. 2021: Provenance and diagenesis of the Upper Miocene sandstones from the Pannonian Basin System. In: Bábek O. & Vodrážková S. (Eds.): Book of Abstract of the 35th IAS Meeting of Sedimentology, Virtual Meeting. Prague, Czech Republic, June 21–25, 2021. Olomouc 2021, 300.

Morton A.C. & Hallsworth C. 2007: Stability of detrital heavy minerals during burial diagenesis. In: Mange M.A. & Wright D.T. (Eds.): *Developments in Sedimentology* 58, 215–245. https://doi.org/10.1016/S0070-4571(07)58007-6

Neubauer T.A., Harzhauser M., Kroh A., Georgopoulou E. & Mandic O. 2015: A gastropod-based biogeographic scheme for the European Neogene freshwater systems. *Earth-Science Reviews* 143, 98–116. https://doi.org/10.1016/j.earscirev.2015.01.010

Nyíri D., Tőkés L., Zadravecz C. & Fodor L. 2021: Early post-rift confined turbidite systems in a supra-detachment basin: Implications for the early to middle Miocene basin evolution and hydrocarbon exploration of the Pannonian Basin. *Global and*

Planetary Change 203, 103500. https://doi.org/10.1016/j.gloplacha.2021.103500

Pamić J. 1986: Magmatic and metamorphic complexes of the adjoining area of the northernmost Dinarides and Pannonian Mass. *Acta Geologica Hungarica* 29, 203–220.

Pamić J. 1999: Kristalinska podloga južnih dijelova Panonskog bazena – temeljena na površinskim i bušotinskim podacima. *Nafta* (Zagreb) 50, 291–310.

Pamić J. & Lanphere M. 1991: Hercinske granitne i metamorfne stijene Papuka, Psunja, Krndije i okolne podloge Panonskog bazena u Slavoniji (sjeverna Hrvatska, Jugoslavija) [Hercynian Granites and Metamorphic Rocks from the Mts. Papuk, Psunj, Krndija and the Surrounding Basement of the Pannonian Basin in slavonija (Northern Croatia, Yugoslavia)]. *Geologija* 34, 81–253 (in Croatian with English Summary).

Pavelić D. 2001: Tectonostratigraphic model for the North Croatian and North Bosnian sector of the Miocene Pannonian Basin System. *Basin Research* 13, 359–376. https://doi.org/10.1046/j.0950-091x.2001.00155.x

Pavelić D. 2005: Cyclicity in the evolution of the Neogene North Croatian basin (Pannonian Basin System). In: Mabessoone J.M. & Neumann V.H. (Eds.): Cyclic Development of Sedimentary Basins. *Developments in Sedimentology* 57, 273–283. https://doi.org/10.1016/S0070-4571(05)80011-1

Pavelić D. & Kovačić M. 2018: Sedimentology and stratigraphy of the Neogene rift-type North Croatian Basin (Pannonian Basin System, Croatia): A review. *Marine and Petroleum Geology* 91, 455–469. https://doi.org/10.1016/j.marpetgeo.2018.01.026

Pavelić D., Miknić M. & Sarkotić Šlat M. 1998: Early to Middle Miocene facies succession in lacustrine and marine environments on the southwestern margin of the Pannonian Basin System (Croatia). *Geologica Carpathica* 49, 433–443.

Pettijohn F.J. 1957: Sedimentary rocks. *Harper & Brothers*, New York.

Pettijohn F.J., Potter P.E. & Siever R. 1987: Sand and sandstone. 2nd edition, *Springer*, New York.

Piller W., Harzhauser M. & Mandic O. 2007: Miocene Central Paratethys stratigraphy – current status and future directions. *Stratigraphy* 4, 151–168.

Pogácsás Gy. 1984: Seismic stratigraphic features of the Neogene sediments in the Pannonian Basin. *Geofizikai Közlemények* 30, 373–410.

Powers M.C. 1953: A new roundness scale for sedimentary particles. *Journal of Sedimentary Research* 23, 117–119. https://doi.org/10.1306/D4269567-2B26-11D7-8648000102C1865D

Prelogović E. 1975: Neotektonska karta SR Hrvatske. *Geološki Vjesnik* 28, 97–108.

Prelogović E., Saftić B., Kuk V., Velić J., Dragaš M. & Lučić D. 1998: Tectonic activity in the Croatian part of the Pannonian basin. *Tectonophysics* 297, 283–293. https://doi.org/10.1016/S0040-1951(98)00173-5

Premec Fućek V., Galović I., Mikša G., Hernitz Kučenjak M., Krizmanić K., Hajek-Tadesse V., Matošević M., Pecimotika G. & Zlatar S. 2022: Paleontological and lithological evidence of the late Karpatian to early Badenian marine succession from Medvednica Mountain (Croatia), Central Paratethys. *International Journal of Earth Sciences*. https://doi.org/10.1007/s00531-022-02264-4

Rahman M.J.J. & Worden R.H. 2016: Diagenesis and its impact on the reservoir quality of Miocene sandstones (Surma Group) from the Bengal Basin, Bangladesh. *Marine and Petroleum Geology* 77, 898–915. https://doi.org/10.1016/j.marpetgeo.2016.07.027

Rögl F. 1998: Paleogeographic considerations for Mediterranean and Paratethys seaways (Oligocene to Miocene). *Annalen des Naturhistorischen Museum in Wien* 99 A, 279–310.

Rögl F. & Steininger F.F. 1983: Vom Zerfall der Tethys zu Mediterran und Paratethys. Die Neogene Palaeogeographie und Palinspastik des zirkum-mediterranen Raumes. *Annalen des Naturhistorischen Museum in Wien* 85 A, 135–163.

Royden L.H. 1988: Late cenozoic tectonics of the Pannonian Basin System. In: Royden L.H. & Horváth F. (Eds.): The Pannonian Basin: A Study in Basin Evolution. *AAPG Memoir* 45, 27–48.

Ružić T. 2021: Geological characterization of the 3D seismic record in the Upper Miocene deposits of the northern part of Bjelovar subdepression. *Dissertation, Faculty of Science, University of Zagreb*.

Rybár S., Kováč M., Šarinová K., Halasova E., Hudáčková N., Šujan M., Kováčová M., Ruman A. & Klučiar T. 2016: Neogene changes in palaeogeography, palaeoenvironment and the provenance of sediment in the Northern Danube Basin. *Bulletin of Geosciences* 91, 367–398.

Rybár S., Šarinová K., Sant K., Kuiper K.F., Kováčová M., Vojtko R., Reiser M.K., Fordinál K., Teodoridis V., Nováková P. & Vlček T. 2019: New $^{40}Ar/^{39}Ar$, fission track and sedimentological data on a middle Miocene tuff occurring in the Vienna Basin: Implications for the north-western Central Paratethys region. *Geologica Carpathica* 70, 386–404. https://doi.org/10.2478/geoca-2019-0022

Saftić B., Velić J., Sztanó O., Juhász Gy. & Ivković Ž. 2003: Tertiary subsurface facies, source rocks and hydrocarbon reservoirs in the SW part of the Pannonian Basin (northern Croatia and south-western Hungary). *Geologia Croatica* 56, 101–122.

Sant K., Kuiper K.F., Rybár S., Grunert, P., Harzhauser M., Mandic O., Jamrich M., Šarinová K., Hudáčková N. & KrijgsmaN W. 2020: $^{40}Ar/^{39}Ar$ geochronology using high sensitivity mass spectrometry: Examples from middle Miocene horizons of the Central Paratethys. *Geologica Carpathica* 71, 166–182. https://doi.org/10.31577/GeolCarp.71.2.5

Šćavničar B. 1979: Pješčenjaci miocena i pliocena Savske potoline. *Znanstveni savjet za naftu Jugosl. akad. znan. i umjet., III. znan. skup sekcije za primj. geol., geofiz. i geokem*., Novi Sad, 1977, 2, 351–383, Zagreb.

Schmid S.M., Bernoulli D., Fügenschuh B., Matenco L., Schefer S., Schuster R., Tischler M. & Ustaszewski K. 2008: The Alpine–Carpathian–Dinaridic orogenic system: correlation and evolution of tectonic units. *Swiss Journal of Geosciences* 101, 139–183. https://doi.org/10.1007/s00015-008-1247-3

Schmid S.M., Fügenschuh B., Kounov A., Matenco L., Nievergelt P., Oberhänsli R., Pleuger J., Schefer S., Schuster R., Tomljenović B., Ustaszewski K. & Van Hinsbergen D.J.J. 2020: Tectonic units of the Alpine collision zone between Eastern Alps and western Turkey. *Gondwana Research* 78, 308–374. https://doi.org/10.1016/j.gr.2019.07.005

Schneider P., Balen D., Opitz J. & Massonne H.J. 2022: Dating and geochemistry of zircon and apatite from rhyolite at the UNESCO geosite Rupnica (Mt. PApuk, northern Croatia) and the relationship to the Sava Zone. *Geologia Croatica* 75, 249–267. https://doi.org/10.4154/gc.2022.19

Sebe K., Kovačić M., Magyar I., Krizmanić K., Špelić M., Bigunac D., Sütő-Szentai M., Kovács Á., Szuromi-Korecz A., Bakrač K., Hajek-Tadesse V., Troskot-Čorbić T. & Sztanó O. 2020: Correlation of upper Miocene–Pliocene Lake Pannon deposits across the Drava Basin, Croatia and Hungary. *Geologia Croatica* 73, 177–195. https://doi.org/10.4154/gc.2020.12

Seghedi I. & Downes H. 2011: Geochemistry and tectonic development of Cenozoic magmatism in the Carpathian–Pannonian region. *Gondwana Research* 20, 655–672. https://doi.org/10.1016/j.gr.2011.06.009

Severin K.P. 2004: Energy dispersive spectrometry of common rock forming minerals. *Kluwer Academic Publishers*, Dordrecht. https://doi.org/10.1007/978-1-4020-2841-0

Sneider R.M. 1990: Reservoir Description of Sandstones. In: Barwis J.H., Mcpherson J.G. & Studlick J.R.J. (Eds.): Sandstone Petroleum Reservoirs. Casebooks in Earth Sciences. *Springer*, New York, 1–3.

Špelić M., Sztanó O., Saftić B. & Bakrač K. 2019: Sedimentary basin fill of Lake Pannon in the eastern part of Drava. In: Horvat M., Matoš B. & Wacha L. (Eds.): Proceedings of the 6th Croatian Geological Congress with international participation. Zagreb, October 9–12, 2019. *Croatian Geological Society*, 192–193.

Sremac J., Bošnjak M., Velić J., Malvić T. & Bakrač K. 2022: Nearshore Pelagic Influence at the SW Margin of the Paratethys Sea – Examples from the Miocene of Croatia. *Geosciences* 12, 120. https://doi.org/10.3390/geosciences12030120

Starijaš B., Gerdes A., Balen D., Tibljaš D. & Finger F. 2010: The Moslavačka Gora crystalline massif in Croatia: a Cretaceous heat dome within remnant Ordovician granitoid crust. *Swiss Journal of Geosciences* 103, 61–82.

Steininger F.F. & Rögl F. 1979: The Paratethys history – a contribution towards the Neogene geodynamics of the Alpine Orogene (an abstract). *Ann. Géol. Pays Hellén.*, Tome hors serie, fasc. III, 1153–1165, Athens.

Šuica S., Garašić V. & Woodland A.B. 2022a: Petrography and geochemistry of granitoids and related rocks from the pre-Neogene basement of the Slavonia–Srijem Depression (Croatia). *Geologia Croatica* 75, 129–144. https://doi.org/10.4154/gc.2022.09

Šuica S., Tapster S.R., Mišur I. & Trinajstić N. 2022b: The Late Cretaceous syenite from the Sava suture zone (eastern Croatia). In: XXII International Congress of the CBGA, Plovdiv, Bulgaria, 7–11 September 2022, Abstracts, 100.

Suttner L.J., Basu A. & Mack G.H. 1981: Climate and the origin of quartz arenites. *Journal of Sedimentary Research* 51, 1235–1246. https://doi.org/10.1306/212F7E73-2B24-11D7-8648000102C1865D

Szentgyörgyi K. & Juhász Gy. 1988: Sedimentological characteristics of the Neogene sequences in SW Transdanubia, Hungary. *Acta Geologica Hungarica* 31, 209–225.

Sztanó O., Szafián P., Magyar I., Horányi A., Bada G., Hughes D.W., Hoyer D.L. & Wallis R.J. 2013: Aggradation and progradation controlled clinothems and deepwater sand delivery model in the Neogene Lake Pannon, Makó Trough, Pannonian Basin, SE Hungary. *Global and Planetary Change* 103, 149–167. https://doi.org/10.1016/j.gloplacha.2012.05.026

Sztanó O., Sebe K., Csillag G. & Magyar I. 2015: Turbidites as indicators of paleotopography, Upper Miocene Lake Pannon, Western Mecsek Mountains (Hungary). *Geologica Carpathica* 66, 331–344. https://doi.org/10.1515/geoca-2015-0029

Tadej J. 2011: Evolution of the Early and Middle Miocene sedimentary environments in the north-western part of the Drava Depression based on the well analysis data. *Dissertation, Faculty of mining, geology and petroleum engineering, University of Zagreb*.

Tari G., Horváth F. & Rumpler J. 1992: Styles of extension in the Pannonian Basin. *Tectonophysics* 208, 203–219. https://doi.org/10.1016/0040-1951(92)90345-7

Tomljenović B. & Csontos L. 2001: Neogene-Quaternary structures in the border zone between Alps, Dinarides and Pannonian Basin (Hrvatsko zagorje and Karlovac basins, Croatia). *International Journal of Earth Sciences* 90, 560–578. https://doi.org/10.1007/s005310000176

Troskot-Čorbić T., Velić J. & Malvić T. 2009: Comparison of the Middle Miocene and the Upper Miocene source rock formations in the Sava Depression (Pannonian Basin, Croatia). *Geologia Croatica* 62, 123–133.

Ustaszewski K., Schmid S.M., Lugović B., Schuster R., Schaltegger U., Bernoulli D., Hottinger L., Kounov A., Fügenschuh B. & Schefer S. 2009: Late Cretaceous intra-oceanic magmatism in the internal Dinarides (northern Bosnia and Herzegovina): Implications for the collision of the Adriatic and European plates. *Lithos* 108, 106–125. https://doi.org/10.1016/j.lithos.2008.09.010

Ustaszewski K., Kounov A., Schmid S.M., Schaltegger U., Krenn E., Frank W. & Fügenschuh B. 2010: Evolution of the Adria-Europe plate boundary in the northern Dinarides: From continent-continent collision to back-arc extension. *Tectonics* 29, TC6017. https://doi.org/10.1029/2010TC002668

Velić J., Malvić T., Cvetković M. & Vrbanac B. 2012: Reservoir geology, hydrocarbon reserves and production in the Croatian part of the Pannonian Basin System. *Geologia Croatica* 65, 91–101. https://doi.org/10.4154/GC.2012.07

von Eynatten H. 2003: Petrography and chemistry of sandstones from the Swiss Molasse Basin: an archive of the Oligocene to Miocene evolution of the Central Alps. *Sedimentology* 50, 703–725. https://doi.org/10.1046/j.1365-3091.2003.00571.x

Vrbanac B., Velić J. & Malvić T. 2010: Sedimentation of deep-water turbidites in the SW part of the Pannonian Basin. *Geologica Carpathica* 61, 55–69. https://doi.org/10.2478/v10096-010-0001-8

Weltje G.J. 2006: Ternary sandstone composition and provenance: an evaluation of the 'Dickinson model'. In: Buccianti A., Mateu-Figueras G. & Pawlowsky-Glahn V. (Eds.): Compositional data analysis in the geosciences: from theory to practice. *Geological Society of London, Special Publications* 264, 79–99. https://doi.org/10.1144/GSL.SP.2006.264.01.07

Weltje G.J. & von Eynatten H. 2004: Quantitative provenance analysis of sediments: review and outlook. *Sedimentary Geology* 171, 1–11. https://doi.org/10.1016/j.sedgeo.2004.05.007

Weltje G.J., Meijer X.D. & De Boer P.L. 1998: Stratigraphic inversion of siliciclastic basin fills: a note on the distinction between supply signals resulting from tectonic and climatic forcing. *Basin Research* 10, 129–153. https://doi.org/10.1046/j.1365-2117.1998.00057.x

Wentworth C.K. 1922: A scale of grade and class terms for clastic sediments. *The Journal of Geology* 30, 377–392.

Willems C.J.L., Cheng C., Watson S.M., Minto J., Williams A., Walls D., Milsch H., Burnside N.M. & Westaway R. 2021: Permeability and mineralogy of the Újfalu Formation, Hungary, from production test and experimental rock characterization: Implications for geothermal heat projects. *Energies* 14, 4332. https://doi.org/10.3390/en14144332

Worden R.H. & Burley S.D. 2003: Sandstone diagenesis: the evolution of sand to stone. In: Burley S.D. & Worden R.H. (Eds.): Sandstone Diagenesis: Recent and Ancient. *International Association of Sedimentologists* 4, 3–44.

Worden R.H., Mayall M.J. & Evans I.J. 1997: Predicting reservoir quality during exploration: lithic grains, porosity and permeability in Tertiary clastic rocks of the South China Sea Basin. *Geological Society of London, Special Publications* 126, 107–115. https://doi.org/10.1144/GSL.SP.1997.126.01.08

Worden R.H., Armitage P.J., Butcher A.R., Churchill J.M., Csoma A.E., Hollis C., Lander R.H. & Omma J.E. 2018: Petroleum reservoir quality prediction: Overview and contrasting approaches from sandstone and carbonate communities. *Geological Society of London, Special Publications* 435, 1–31. https://doi.org/10.1144/SP435.21

Zečević M., Velić J., Sremac J., Troskot-Čorbić T. & Garašić V. 2010: Significance of the Badenian petroleum source rocks from Krndija Mt. (Pannonian Basin, Croatia). *Geologia Croatica* 63, 225–239.

Zuffa G.G. 1985: Optical analyses of arenites: influence of methodology on compositional results. In: Zuffa G.G. (Ed.): Provenance of arenites. *Reidel*, Dordrecht, *NATO ASI Series* 148,165–189.

Electronic supplementary material is available online at http://geologicacarpathica.com/data/files/supplements/GC-74-2-Matosevic_Supplement.xlsx